

Fatty acid elongase-5 (Elovl5) regulates hepatic triglyceride catabolism in obese C57BL/6J mice[§]

Sasmita Tripathy,* Kelli A. Lytle,* Robert D. Stevens,[†] James R. Bain,[†] Christopher B. Newgard,[†] Andrew S. Greenberg,[§] Li-Shin Huang,** and Donald B. Jump^{1,*}

School of Biological and Population Health Sciences and the Linus Pauling Institute,* Oregon State University, Corvallis, OR 97331; Sarah W. Stedman Nutrition and Metabolism Center,[†] Duke University Medical Center, Durham, NC 27710; Obesity and Metabolism Laboratory,[§] Jean Mayer USDA Human Nutrition Research Center, Boston, MA 02111; and Department of Medicine,** Columbia University College of Physicians & Surgeons, New York, NY 10032

Abstract Nonalcoholic fatty liver disease is a major public health concern in the obese and type 2 diabetic populations. The high-fat lard diet induces obesity and fatty liver in C57BL/6J mice and suppresses expression of the PPAR-target gene, FA elongase 5 (Elovl5). Elovl5 plays a key role in MUFA and PUFA synthesis. Increasing hepatic Elovl5 activity in obese mice lowered hepatic TGs and endoplasmic reticulum stress markers (X-box binding protein 1 and cAMP-dependent transcription factor 6 α) and increased TG catabolism and fatty acyl carnitines. Increased hepatic Elovl5 activity did not increase hepatic capacity for β -oxidation. Elovl5 effects on hepatic TG catabolism were linked to increased protein levels of adipocyte TG lipase (ATGL) and comparative gene identification 58 (CGI58). Elevated hepatic Elovl5 activity also induced the expression of some (pyruvate dehydrogenase kinase 4 and fibroblast growth factor 21), but not other cytochrome P450 4A10 (CYP4A10), PPAR-target genes. FA products of Elovl5 activity increased ATGL, but not CGI58, mRNA through PPAR β -dependent mechanisms in human HepG2 cells. Treatment of mouse AML12 hepatocytes with the PPAR β agonist (GW0742) decreased ¹⁴C-18:2,n-6 in TGs but did not affect β -oxidation. **¶** These studies establish that Elovl5 activity regulates hepatic levels of FAs controlling PPAR β activity, ATGL expression, and TG catabolism, but not FA oxidation.—Tripathy, S., K. A. Lytle, R. D. Stevens, J. R. Bain, C. B. Newgard, A. S. Greenberg, L.-S. Huang, and D. B. Jump. Fatty acid elongase-5 (Elovl5) regulates hepatic triglyceride catabolism in obese C57BL/6J mice. *J. Lipid Res.* 2014. 55: 1448–1464.

Supplementary key words fatty liver • adipocyte triglyceride lipase • pyruvate dehydrogenase kinase 4 • peroxisome proliferator-activated receptor β • fatty acid oxidation

Nonalcoholic fatty liver disease (NAFLD) is a significant public health concern for the obese and type 2 diabetic

populations. NAFLD is the hepatic manifestation of metabolic syndrome and is associated with a cluster of metabolic risk factors including obesity, dyslipidemia, type 2 diabetes, and hypertension (1). The prevalence of NAFLD is ~30% in US adults but is as high as 90–95% in obese individuals and $\geq 60\%$ in type 2 diabetic subjects (2). NAFLD is viewed as a pathological spectrum with benign fatty liver at one end and nonalcoholic steatohepatitis (NASH; inflammation, oxidative stress, hepatic damage, and fibrosis) at the other end (1). Thirty to 40% of individuals with simple fatty liver develop NASH, which can progress to cirrhosis, a risk factor for hepatic cancer (3).

NAFLD involves excessive neutral lipid storage in the liver as TG, cholesteryl ester, and diacylglycerol (DAG) (4–6). NEFAs used for TG synthesis are derived from multiple sources including those mobilized from adipose tissue,

Abbreviations: AADAC, arylacetamide deacetylase; ABHD5, α/β -hydrolase fold domain-containing protein 5; Ad-ATGL, adenovirus expressing ATGL; Ad-Elovl5, adenovirus expressing Elovl5; Ad-Luc, adenovirus expressing luciferase; ADPN, adiponutrin; Ad-shRNA-ATGL, adenovirus expressing shRNA-ATGL; Ad-shRNA-scrambled, adenovirus expressing shRNA-scrambled; Akt, thymoma viral proto-oncogene; ARA, arachidonic acid; ASM, acid soluble material; ATF6 α , cAMP-dependent transcription factor 6 α ; ATGL, adipocyte TG lipase; CES, carboxylesterase; CGI58, comparative gene identification 58; *cis*-VA, *cis*-vaccenic acid; CPT, carnitine palmitoyl transferase; DIO, diet-induced obesity; DNL, de novo lipogenesis; Elovl, FA elongase; ER, endoplasmic reticulum; FADS1, FA desaturase 1 (Δ^5 -FA desaturase); FADS2, FA desaturase 2 (Δ^6 -FA desaturase); FAO, FA oxidation; FGF21, fibroblast growth factor 21; FoxO1, forkhead box O1; GNG, gluconeogenesis; HFD, high-fat diet; HSD, honestly significant difference; HTG, hepatic TG; LCAD, long-chain acyl-CoA dehydrogenase; LFD, low-fat diet; MCAD, medium-chain acyl-CoA dehydrogenase; mTORC, mammalian target of rapamycin complex; NAFLD, nonalcoholic fatty liver disease; PDE1 α , pyruvate dehydrogenase E1 α ; PDK4, pyruvate dehydrogenase kinase 4; PKC, protein kinase C; PNPLA, patatin-like phospholipase domain containing; qRT-PCR, quantitative RT-PCR; SCAD, short-chain acyl-CoA dehydrogenase; SCD1, stearoyl-CoA desaturase 1; SFA, saturated FA; SIRT3, sirtuin 3; SREBP1, sterol-regulatory element binding protein 1; TBP, TATA binding protein; TGH, TG hydrolase; XBP1, X-box binding protein 1.

¹To whom correspondence should be addressed.

e-mail: Donald.Jump@oregonstate.edu

[§]The online version of this article (available at <http://www.jlr.org>) contains supplementary data in the form of one table and five figures.

This work was supported the USDA National Institute of Food and Agriculture Grant 2009-65200-05846 and the National Institutes of Health Grants DK043220 (D.B.J.), DK094600 (D.B.J.), and AA020561 (L.-S.H.).

Manuscript received 9 April 2014 and in revised form 8 May 2014.

Published, JLR Papers in Press, May 9, 2014

DOI 10.1194/jlr.M050062

generated by de novo lipogenesis (DNL), or recovered from portal circulation. Hepatic TG (HTG) hydrolysis provides NEFA substrates for FA oxidation (FAO) and VLDL assembly and secretion (4, 7). Fatty liver develops when there is an imbalance in these pathways. Recent rodent studies suggest that fatty liver maybe associated with problems in unsaturated FA metabolism (8–13).

We previously reported that FA elongase (Elovl) 5, a key PPAR α -regulated enzyme involved in MUFA and PUFA synthesis, was suppressed in fatty livers of diet-induced obese (DIO) mice (14, 15). A modest 2-fold increase in hepatic Elovl5 activity in obese mice reduced HTG content to levels seen in lean mice. Hepatic cholesterol and fasting plasma TG levels, however, were not affected by changes in Elovl5 activity.

Elovl5 is one of seven Elovl subtypes expressed in humans and rodents. Using malonyl CoA, NADPH, and fatty acyl-CoA as substrates, Elovl5 and its associated enzymes (3-keto CoA reductase, 3-hydroxyacyl CoA dehydrase, and *trans*-2,3-enoyl CoA reductase) catalyze two-carbon additions to both MUFAs and PUFAs. Elovl5 plays a key role in the synthesis of C₂₀ n-6 PUFAs [e.g., arachidonic acid (ARA), 20:4,n-6] and C₂₂ n-3 PUFAs (e.g., DHA, 22:6,n-3), as well as the n-7 class of MUFAs, specifically, *cis*-vaccenic acid (*cis*-VA, 18:1,n-7). Elovl5, however, does not elongate saturated FAs (SFAs) or the n-9 class of MUFAs (15–17).

Our previous studies established that hepatic Elovl5 activity was inversely associated with TG content, blood glucose, and hepatic expression of enzymes involved in gluconeogenesis (GNG) (14, 15, 18). While the mechanism for Elovl5 control of blood glucose and GNG was linked to *cis*-VA synthesis and its regulation of the mammalian target of rapamycin complex 2-thymoma viral proto-oncogene-forkhead box O1 (mTORC2-AKT-FoxO1) pathway (14, 19), the mechanism for Elovl5 control of HTG is unknown.

This report examined mechanisms to explain how changes in hepatic Elovl5 activity regulate TG content. Using a DIO mouse model (14, 15), we established that Elovl5 regulates HTG content by controlling the abundance of adipocyte TG lipase (ATGL), also known as patatin-like phospholipase domain-containing (PNPLA) 2, and its coregulator, comparative gene identification 58 [CGI58, also known as α/β -hydrolase fold domain-containing protein 5 (ABHD5)] (20). DIO suppressed hepatic FAO and the expression of multiple PPAR-regulated genes. While elevated Elovl5 activity did not increase the capacity of the liver to β -oxidize FAs, Elovl5 activity increased hepatic levels of key PUFAs that activated PPAR signaling and induced ATGL.

MATERIALS AND METHODS

Materials

DMEM with high glucose (25 mM), DMEM/F12 medium, and antibiotics for cell culture were obtained from Invitrogen. Hyclone fetal calf serum was purchased from Thermo-Fisher Scientific. Transferrin, sodium selenite, sodium ascorbate, and HEPES were purchased from Sigma Chemical Co. Chemical agonists for PPAR α , PPAR β , and PPAR γ (i.e., WY14643, GW0742, and pioglitazone,

respectively) and antagonists (i.e., GW6471, GSK3787, and T0070907, respectively) were obtained from Tocris Bioscience (Bristol, UK). ¹⁴C-labeled FAs were obtained from Amersham Radiochemicals (¹⁴C-palmitate), Perkin Elmer (¹⁴C-oleate and ¹⁴C-linolenate), and American Radiolabeled Chemicals (¹⁴C-*cis*-vaccenate). Antibodies against ATGL were obtained from Cell Signaling (Danvers, MA). Antibodies against CGI58 (ABHD5), X-box binding protein 1 (XBPI), cAMP-dependent transcription factor 6 α (ATF6 α), and Na,K-ATPase were purchased from Santa Cruz Biotechnology (Santa Cruz, CA). The TATA-binding protein (TBP) antibody was obtained from Abcam (Cambridge, MA). The antibodies against calnexin, pyruvate dehydrogenase E1 α (PDE1 α), phospho-S²⁹³-PDE1 α , phospho-S³⁰⁰-PDE1 α , pyruvate dehydrogenase kinase 4 (PDK4), and vinculin were purchased from Millipore/EMD. The secondary antibodies, IRDye 680 and IRDye 800 (anti-mouse, anti-rabbit, and anti-goat), were obtained from LiCor Inc. (Lincoln, NE).

Recombinant adenovirus

The source, construction, purification, titration, and use of the recombinant adenovirus expressing luciferase (Ad-Luc) and Elovl5 (Ad-Elovl5) was described previously (14, 15). Construction of adenovirus expressing ATGL (Ad-ATGL), shRNA-ATGL (Ad-shRNA-ATGL), and shRNA-scrambled (Ad-shRNA-scrambled) were described previously (5, 21).

Dietary manipulation and adenoviral infection of mice

All procedures for the use and care of animals for laboratory research were approved by the Institutional Animal Care and Use Committee at Oregon State University. Male C57BL/6J mice were fed a low-fat diet (LFD: 10% calories as fat diet; Research Diets, D12450B) or a high-fat diet (HFD: 60% calories as fat diet; Research Diets, D12492) for 12 weeks (14). After 12 weeks on these diets, mice fed the LFD were lean and euglycemic; whereas mice fed the HFD were obese, hyperglycemic, glucose intolerant, and insulin resistant and had fatty liver. Five days prior to termination of the experiment, mice were infected with Ad-Luc or Ad-Elovl5. Five days later, mice were fasted overnight; half of the fasted mice were refed their diets for 4 h. Fasted and refed mice were euthanized at 8 AM and 12 noon for the recovery of blood and liver. Most data reported here are from fasted mice; the supplementary data contains data from fasted and refed mice. Methods for liver recovery and preparation of protein and RNA extracts were described previously (14).

Immunoblot analysis of proteins

Proteins were extracted from mouse liver, AML12 cells, and HepG2 cells for immunoblotting as described previously (14, 18, 19). Loading controls for immunoblotting included Na,K-ATPase, calnexin, vinculin, and TBP.

RNA extraction and quantitative real-time PCR

Total RNA was extracted from mouse liver, AML12, and HepG2 cells using TRIzol (Invitrogen), and transcript levels were measured by quantitative RT-PCR (qRT-PCR) as described (14, 19). Gene-specific primers are listed in (supplementary Table 1). All primer pairs were assessed for reaction efficiency and product size; all reactions were performed in triplicate. The relative amounts of mRNAs were calculated by using the comparative CT method (User Bulletin #2, Applied Biosystems, Carlsbad, CA). Cyclophilin was used as a control for these studies (22).

Measurement of plasma β -hydroxybutyrate and HTG

The methods for measurement of plasma β -hydroxybutyrate and HTG contents were described previously (14).

Targeted metabolomic analysis of hepatic acyl carnitines

Targeted metabolomic analysis was performed using fasted livers from obese mice. This analysis was carried out at the Sarah W. Stedman Nutrition and Metabolism Center, Duke University Medical Center. Hepatic fatty acyl carnitines were quantified as described previously (23, 24).

Ex vivo FAO assay in liver

FAO in mouse liver samples used the methods described by others (25, 26) with minor modifications. Briefly, livers (~25 mg) were homogenized in 1 ml of the homogenization buffer containing 100 mM sucrose; 10 mM Tris-HCl, pH 7.5; 5 mM potassium phosphate; 80 mM potassium chloride; 1 mM magnesium chloride; and protease inhibitors (cOmplete, Mini, EDTA-free; Roche). Protein was quantified by Quick Start Bradford Dye Reagent from Bio-Rad (Hercules, CA). The final reaction mix contained the following: 100 mM sucrose; 10 mM Tris-HCl, pH 7.5; 5 mM potassium phosphate; 80 mM potassium chloride; 1 mM magnesium chloride; 2 mM L-carnitine; 0.125 mM malate; 2 mM ATP; 0.2 mM CoA; 0.05 mM DTT; 0.2 mM EDTA; 0.3% BSA; 100 μ M 18:2,n-6; 0.2 μ Ci 14 C-18:2,n-6/reaction; and ~100 μ g protein/reaction in a total volume of 200 μ l. The reaction was run at 30°C for 1 h in screw-capped microfuge tubes. The reaction was stopped with 40 μ l of 60% perchloric acid and mixing. Total and acid soluble 14 C was quantified by β -scintillation counting as described (22), and the results were expressed as nanomoles of acid soluble material (ASM) per milligram of protein.

The method for FAO analysis in HepG2 and AML12 cells was described previously (22). Assays used 14 C-18:2,n-6 as the substrate for FAO; results are expressed as nanomoles of ASM per milligram of protein. Cell protein was measured using the Quick Start Bradford Dye Reagent from Bio-Rad.

Ex vivo measurement of HTG hydrolysis

TG hydrolysis was measured according to procedures reported by others (5, 27, 28) with minor modifications. Briefly, ~100 mg of liver was homogenized in Buffer A1 (0.25 M sucrose, 1 mM EDTA, 1 mM DTT, and containing protease inhibitors). Homogenates were centrifuged at 28,700 rpm in an SW50.1TI rotor (100,000 g) for 1 h at 4°C. The delipidated homogenate was recovered and assayed for TG hydrolysis. The substrate for TG hydrolysis was prepared as described (5, 27, 28) with minor modifications. Briefly, 0.5 μ Ci 14 C-triolein (NEC674L, PerkinElmer; 14 C was carbon 1 of the oleic acid acyl chain), 2.5 μ mol of triolein (NuChek Prep), and 640 nmol of phosphatidyl choline (Avanti Polar Lipids) were added to a glass tube and dried under nitrogen. Lipids were resuspended in 0.75 ml of TNE buffer (20 mM Tris-Cl, pH 7.5; 0.15 M NaCl; and 1 mM EDTA), the sample was vigorously vortexed to create an emulsion, 0.6 ml of the Buffer A1 and 0.15 ml of 20% BSA (in Buffer A1) were added, and the suspension was vigorously vortexed again.

The TG hydrolysis reaction mix was in a final volume of 200 μ l and contained 200 μ g of hepatic protein, 167 nmol of triolein; 50 nCi of 14 C-triolein and 43 nmol phosphatidyl choline. The reaction was run at 37°C for 2 h with intermittent mixing. Reaction products were extracted in chloroform-methanol (2:1), dried under nitrogen, and resuspended in chloroform. Reaction products were fractionated into neutral lipids (tri-, di-, and monoacylglycerides) and NEFAs using an aminopropyl column (Alltech) as described previously (29, 30). The neutral lipid and NEFA fractions were dried under nitrogen and resuspended in 100 μ l of chloroform, and the radioactivity was quantified by β -scintillation counting. Results are reported as nanomoles oleic acid released per milligram of protein per hour.

HepG2 and AML12 cell culture

Human HepG2 hepatoma cells (CRL11997) and mouse AML12 hepatocytes (CRL2254) were obtained from American Type Culture Collection (Manassas, VA). HepG2 cells were grown in DMEM with 25 mM glucose media with 10% fetal calf serum. AML12 cells were grown in DMEM/F12 with fetal calf serum (10%), insulin (1 μ M), dexamethasone (200 nM), transferrin (6 μ g/ml), selenium (6 ng/ml), ascorbate (100 μ M), and HEPES, pH 7.4 (25 mM). All media contained antibiotics (penicillin and streptomycin), and all experiments were carried out in cells grown on 6-well plates (Corning Life Sciences, Corning, NY) in a humidified incubator at 37°C and 5% CO₂. AML12 and HepG2 cells were infected with recombinant adenovirus expressing either a control virus (Ad-shRNA-scrambled) or test viruses (Ad-ATGL and Ad-shRNA-ATGL) at 20 infectious units (IU) per cell. Analysis of 14 C-18:2,n-6 uptake, assimilation into complex lipids, and FAO used methods described previously (22).

Statistical analysis

Statistical analyses used StatView statistical software and the VassarStats website (<http://vassarstats.net/>). Specific analyses included one-way and two-way ANOVA plus the post hoc Tukey test for honestly significant difference (HSD). Student's *t*-test was also used. Data are expressed as mean \pm SD; *P* \leq 0.05 was considered statistically different.

RESULTS

Elovl5 activity regulates HTG content and endoplasmic reticulum stress

C57BL/6J mice fed an HFD (60% energy as fat) develop fatty liver as reflected by a ~2-fold increase in HTG (Fig. 1A). These mice also have 60% lower plasma β -hydroxybutyrate, when compared with LFD-fed (10% energy as fat) mice, suggesting a problem with hepatic FAO (Fig. 1B). Fatty liver in HFD-fed mice is also associated with increased nuclear content of two endoplasmic reticulum (ER) stress markers (31, 32), that is, XBP1 (3-fold) and ATF6 α (1.8-fold) (Fig. 2).

The HFD lowered hepatic Elovl5 mRNA, protein, and activity by ~40%, while Ad-Elovl5 infection of HFD-fed mice increased Elovl5 protein and activity by ~2-fold (14). Increased hepatic Elovl5 activity was associated with a reduction of HTG and an increase in plasma β -hydroxybutyrate to levels seen in lean LFD-fed mice (Fig. 1). These parameters were significantly affected by an interaction between diet (LFD vs. HFD) and genotype (Ad-Luc vs. Ad-Elovl5). While ER-stress markers were significantly reduced in both lean and obese mice infected with Ad-Elovl5 (Fig. 2), there was no significant interaction between diet and genotype. Changes in ER-stress markers were associated with changes in Elovl5 expression (genotype).

Increasing hepatic Elovl5 activity in lean or obese mice had no effect on food intake, body weight, plasma TGs or NEFAs, or hepatic cholesterol content (14, 18). Increased hepatic Elovl5 also did not impair the fast-feed response of glycerol-3-phosphate acyltransferase-1 (GPAT1) or affect hepatic microsomal TG transport protein mRNA abundance (supplementary Figs. I, II). These findings suggest that

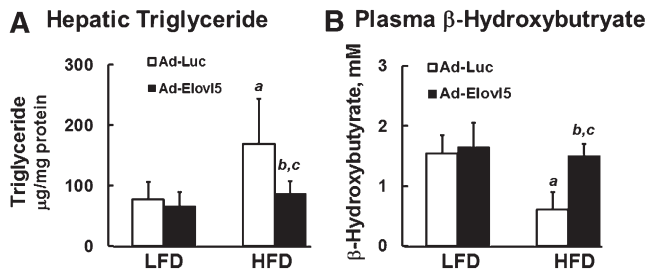


Fig. 1. Elevated Elov15 activity decreases HTG and increases plasma β -hydroxybutyrate in DIO mice. HTG (A) and plasma β -hydroxybutyrate (B) were measured in fasted lean and obese mice maintained on an LFD or an HFD for 12 weeks. Mice were infected with either Ad-Luc or Ad-Elov15 (Materials and Methods). Measurement of HTG and plasma β -hydroxybutyrate was previously described (14). Results are from two separate studies and are expressed as mean \pm SD, $n = 6$. *a*, $P \leq 0.05$ versus Ad-Luc-infected mice on the LFD (diet effect); *b*, $P \leq 0.05$ versus Ad-Luc-infected mice fed the LFD or HFD (genotype effect); *c*, $P \leq 0.05$, interaction between diet (LFD vs. HFD) and genotype (Ad-Luc vs. Ad-Elov15); two-way ANOVA with post hoc HSD test.

Elov15 regulates HTG content through pathways controlling TG catabolism and/or FAO.

Impact of diet and Elov15 on FAO in lean and obese mice

The effects of diet and Elov15 on FAO were investigated using hepatic extracts to measure the formation of ^{14}C -labeled ASM generated from ^{14}C -18:2,n-6 (Fig. 3); ASM is a measure of FAO. The HFD lowered hepatic FAO by $\sim 50\%$, which is in agreement with other reports (25). Elevated hepatic Elov15 activity did not increase β -oxidation of ^{14}C -18:2,n-6 in LFD- or HFD-fed mice (Fig. 3A).

While the HFD did not affect PDK4 expression, PDK4 mRNA was significantly induced 2.5- and 6-fold, respectively, in LFD- and HFD-fed mice infected with Ad-Elov15. The HFD had no significant effect on the expression of enzymes involved in fatty acyl carnitine metabolism [carnitine palmitoyl transferase (CPT) 1a and CPT2], mitochondrial β -oxidation [long-chain acyl-CoA dehydrogenase (LCAD), medium-chain acyl-CoA dehydrogenase (MCAD), and short-chain acyl-CoA dehydrogenase (SCAD)], or sirtuin 3 (SIRT3), an NAD^+ -regulated deacetylase implicated in the control of FAO (25, 33–47) (Fig. 3B). Increased Elov15 activity, however, significantly (~ 2 -fold) increased CPT2, LCAD, and MCAD in livers of obese mice.

The impact of Elov15 on PDK4 expression was examined further because of the role PDK4 plays in regulating mitochondrial substrate utilization. Increased PDK4 activity is associated with decreased carbohydrate and increased FA utilization by mitochondria (48–50). PDK4 phosphorylates a key regulatory subunit of pyruvate dehydrogenase (i.e., PDE1 α). Phosphorylation of PDE1 α inhibits pyruvate dehydrogenase activity leading to increased mitochondrial utilization of FAs for oxidation. We quantified the level of PDK4 and PDE1 α protein, as well as PDE1 α phosphorylation at two regulatory sites, S^{293} -PDE1 α and S^{300} -PDE1 α (Fig. 4). Diet did not significantly affect PDK4, total PDE1 α protein abundance, or the phosphorylation status of PDE1 α at S^{293} or S^{300} . Elevated Elov15 activity, however, significantly lowered PDK4 protein abundance ($\geq 50\%$) in both the LFD- and HFD-fed mice. The decline in PDK4 protein is in contrast with the effect of Elov15 on PDK4 mRNA (Fig. 3) and likely represents a posttranslational regulatory mechanism controlled by Elov15.

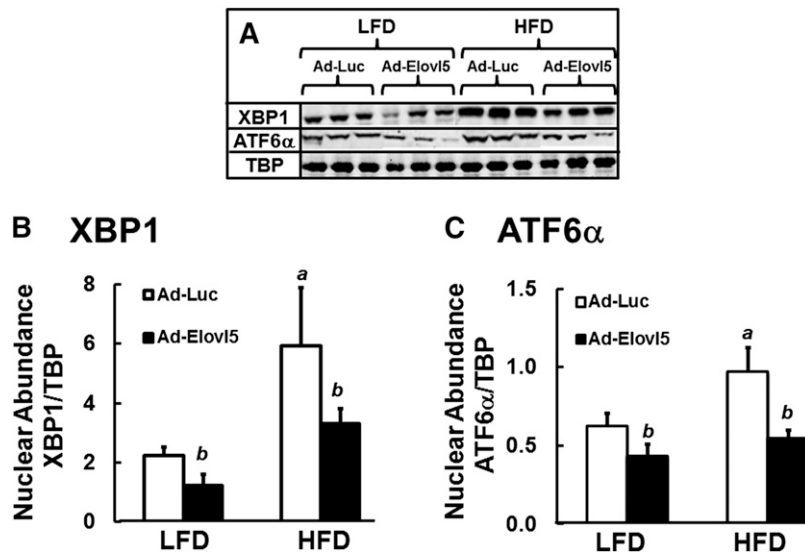


Fig. 2. Elevated Elov15 activity suppresses markers of hepatic ER stress in fasted lean and obese mice. Hepatic extracts from fasted lean (LFD) and obese (HFD) mice infected with either Ad-Luc or Ad-Elov15 were prepared and examined for nuclear protein abundance of XBP1 and ATF6 α (Materials and Methods). A: Representative immunoblots, $n = 3$ mice per group. B and C: Quantified levels of nuclear protein abundance of XBP1 (B) and ATF6 α (C) relative to loading control, TBP. Results are presented as nuclear abundance; the results are from two separate studies and expressed as mean \pm SD, $n = 6$. *a*, $P \leq 0.05$ versus Ad-Luc-infected mice on the LFD (diet effect); *b*, $P \leq 0.05$ versus Ad-Luc-infected mice on the LFD or HFD (genotype effect); two-way ANOVA with post hoc HSD test.

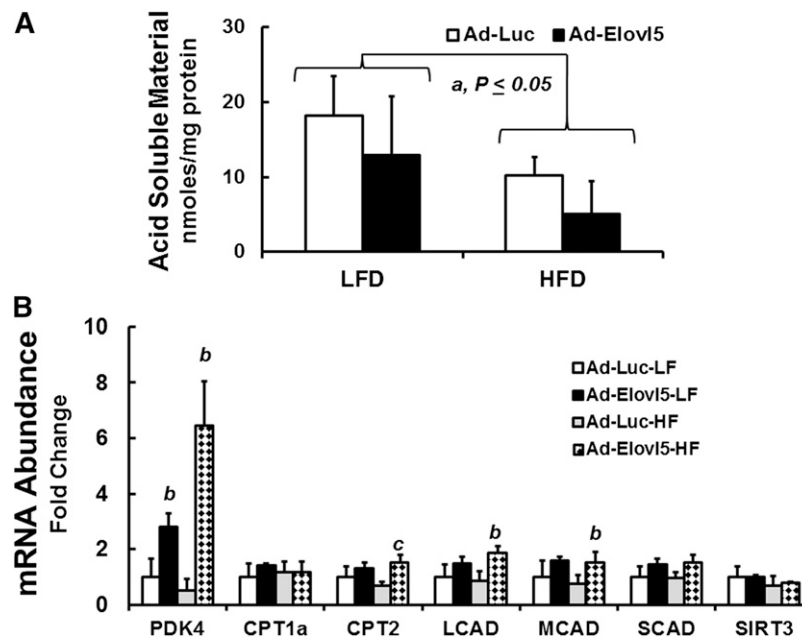


Fig. 3. Impact of obesity and elevated Elovl5 activity on hepatic FAO and the expression of proteins involved in mitochondrial FAO. A: FAO was measured in liver extracts of LFD- and HFD-fed mice infected with either Ad-Luc or Ad-Elovl5 as described (Materials and Methods). Results are expressed as mean \pm SD, $n = 4$ /group. *a*, $P \leq 0.05$ versus Ad-Luc-infected mice fed the LFD; Student's *t*-test. B: Mouse liver RNA extracted from fasted lean low-fat (LF) and obese high-fat (HF) fed mice infected with either Ad-Luc or Ad-Elovl5 was used to quantify mRNAs encoding CPT1a, CPT2, LCAD, MCAD, SCAD, PDK4, and SIRT3 relative to the housekeeping gene cyclophilin (14). Results are presented as mRNA abundance fold change; values are relative to the level of transcript abundance in livers of fasted LFD-fed Ad-Luc-infected mice. *a*, $P \leq 0.05$ versus Ad-Luc-infected mice on the LFD (diet effect); *b*, $P \leq 0.05$ versus Ad-Luc-infected mice fed the LFD or HFD (genotype effect); *c*, $P \leq 0.05$, interaction between diet (LFD vs. HFD) and genotype (Ad-Luc vs. Ad-Elovl5); two-way ANOVA with post hoc HSD test.

Elevated Elovl5 activity had no effect on the phosphorylation of S²⁹³-PDE1 α in either LFD- or HFD-fed mice and modestly induced S³⁰⁰-PDE1 α phosphorylation in LFD-fed mice only (Fig. 4C, D). The effect of elevated Elovl5 activity on PDK4 protein abundance and the lack of significant Elovl5 control of PDE1 α phosphorylation status, a surrogate of pyruvate dehydrogenase activity, argue against products of Elovl5 activity controlling hepatic β -oxidation or mitochondrial substrate utilization.

Elevated Elovl5 activity increases hepatic fatty acyl carnitines

To gain further insight into how Elovl5 regulates HTG content, we carried out a targeted metabolomic analysis to quantify fatty acyl carnitines in livers obtained from fasted obese mice. This analysis provided a second and independent approach to examine β -oxidation of hepatic FAs. The analysis identified multiple fatty acyl carnitines in livers of fasted obese mice; acyl chains ranged in size from 2 to 22 carbons and included acyl carnitines derived from SFAs, MUFAs, and PUFAs (Fig. 5). More importantly, livers derived from obese mice with elevated Elovl5 activity had significantly higher levels of nearly all fatty acyl carnitines. Because Elovl5 had no effect on plasma NEFAs and TGs (14) or hepatic β -oxidation (Fig. 3), these results suggest that increased hepatic FA acyl carnitines were derived

from increased substrate availability for mitochondrial β -oxidation. The likely source of these FAs is the catabolism of stored lipid (e.g., TGs and/or cholesteryl esters).

Elevated hepatic Elovl5 activity increases TG catabolism and the expression of enzymes involved in TG hydrolysis

TG catabolism was quantified in hepatic extracts prepared from LFD- and HFD-fed mice using ¹⁴C-triolein as substrate. While diet did not affect the release of ¹⁴C-oleic acid from ¹⁴C-triolein in hepatic extracts, elevated Elovl5 activity increased ¹⁴C-oleic acid released from ¹⁴C-triolein by ≥ 2 -fold (Fig. 6A).

We next examined the effect of diet and Elovl5 on the expression of several enzymes involved in HTG catabolism. Livers with elevated Elovl5 activity had a ~ 2 -fold higher expression of ATGL and significantly ($>60\%$) lower TG hydrolase [TGH, also known as carboxylesterase 3 (Ces3)] expression. Elevated Elovl5 activity, however, had no significant effect on hepatic mRNAs encoding CGI58, adiponutrin (ADPN, also known as PNPLA3), or arylacetamide deacetylase (AADAC) (Fig. 6B).

Elovl5 increased ATGL protein ≥ 2 -fold in both LFD- and HFD-fed mice (Fig. 6C, D). The level of ATGL protein in HFD-fed mice infected with Ad-Elovl5, however, was not significantly different than ATGL in livers of LFD-fed Ad-Luc-infected mice. In contrast to the results in Fig. 6B,

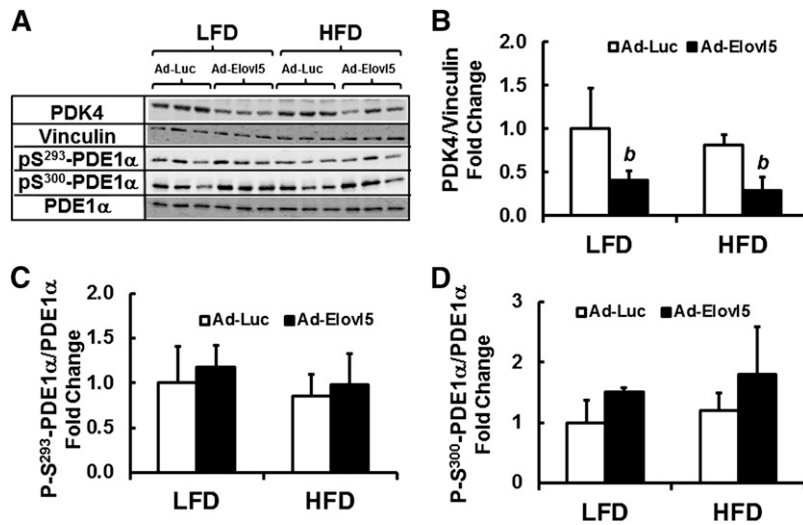


Fig. 4. Effect of diet and Elov5 on PDE1 α phosphorylation. Postnuclear protein extracts from livers of LFD- and HFD-fed mice infected with either Ad-Luc or Ad-Elov5 were assayed for total and phospho-PDE1 α ; two phosphorylation sites on PDE1 α were assessed, S²⁹³ and S³⁰⁰. A: Representative blot with extracts from three separate mice in each group. B–D: Represent the quantitation of these and other immunoblots. Results are represented as mean \pm SD, $n = 4$. *b*, $P \leq 0.05$ versus Ad-Luc-infected mice fed the LFD or HFD (genotype effect); two-way ANOVA with post hoc HSD test.

CGI58 protein abundance was significantly (≥ 2 -fold) higher in livers of LFD- and HFD-fed mice expressing elevated Elov5 (Fig. 6C, E). This outcome suggests that Elov5 activity controls CGI58 protein levels through a posttranslational pathway. This outcome suggests that the combination of increased ATGL and CGI58 protein likely accounts for the elevated TG catabolism in livers of HFD-fed Ad-Elov5-infected mice (Fig. 6A). TGH/CES3 protein abundance was not measured because a decline in the expression of TGH is not consistent with increased TG catabolism.

Impact of diet and Elov5 activity on hepatic gene expression

ATGL protein is $\sim 50\%$ lower in livers of HFD-fed mice than LFD-fed mice (Fig. 6C). Recent studies indicate that reduced or absent cellular ATGL is associated with impaired PPAR signaling (51–53). Elov5 is a PPAR α -target gene, and the HFD knocks down both Elov5 and ATGL expression. Elov5 activity plays a key role in long-chain MUFA and PUFA synthesis (14, 15, 18). Moreover, SFAs, MUFAs, and PUFAs are established PPAR α , β , and γ ligands;

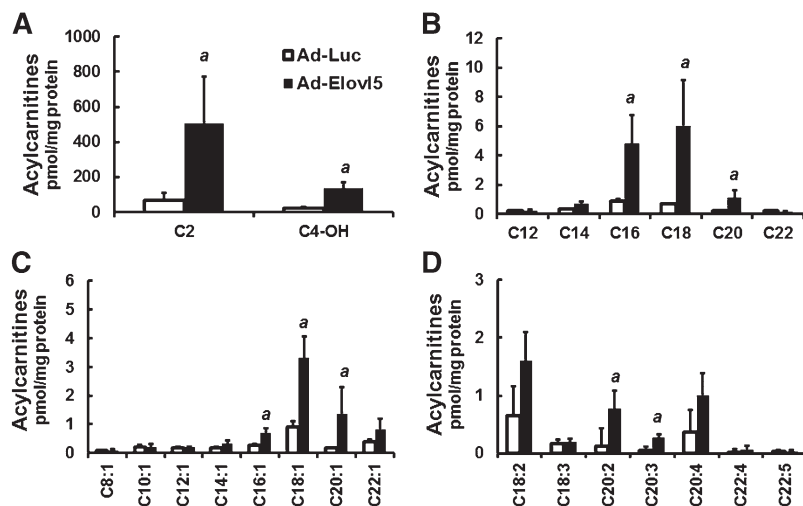


Fig. 5. Elevated Elov5 activity increases hepatic fatty acyl carnitines in fasted obese mice. Hepatic acyl carnitines were extracted from livers of HFD-fed obese mice infected with either Ad-Luc or Ad-Elov5 and quantified using an LC/MS approach described previously (23, 24). A: Hepatic C_{2–4} fatty acyl carnitines of HFD-fed obese mice infected with either Ad-Luc or Ad-Elov5. B: Hepatic C_{12–24} saturated fatty acyl carnitines of fasted HFD-fed obese mice infected with either Ad-Luc or Ad-Elov5. C: Hepatic C_{8–22} monounsaturated fatty acyl carnitines of fasted HFD-fed obese mice infected with either Ad-Luc or Ad-Elov5. D: Hepatic C_{18–22} polyunsaturated fatty acyl carnitines of fasted HFD-fed obese mice infected with either Ad-Luc or Ad-Elov5. Results are normalized to total hepatic protein and expressed as picomoles acyl carnitine per milligram of protein; mean \pm SD, $n = 4$; *a*, $P \leq 0.05$ versus Ad-Luc-infected obese mice; Student's *t*-test.

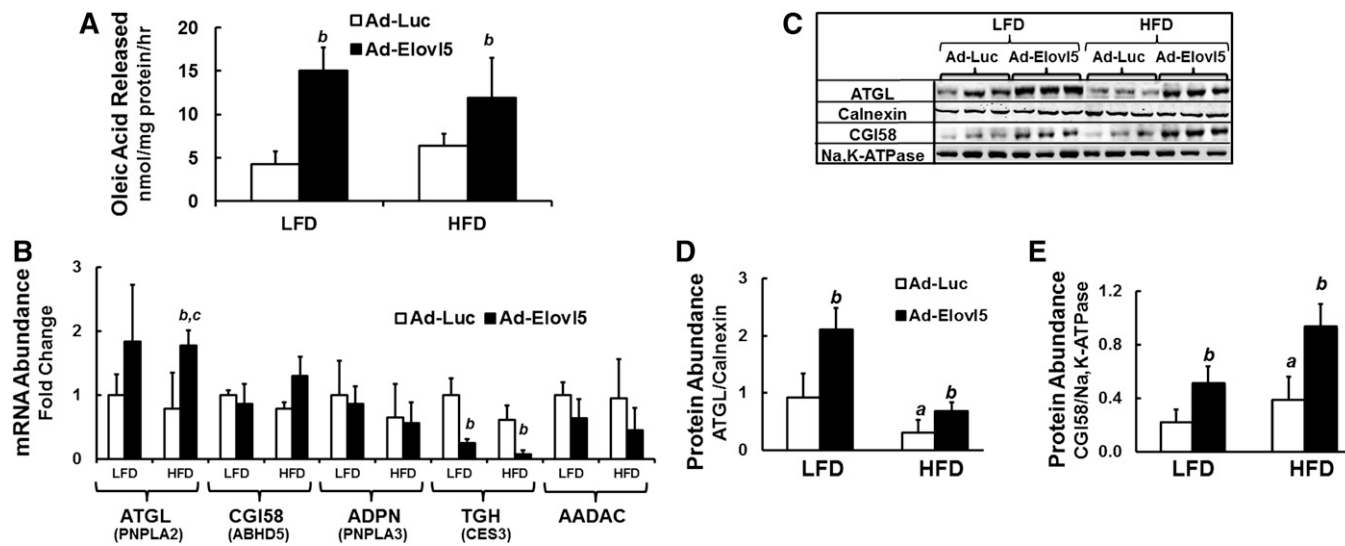


Fig. 6. Elevated Elovl5 activity increases hepatic TG hydrolysis in livers of lean and obese mice. **A:** Hepatic TG hydrolysis. Hepatic cytosolic extracts from fasted LFD- and HFD-fed mice infected with either Ad-Luc or Ad-Elovl5 were measured for TG hydrolyase activity as described (Materials and Methods). Assays were performed in triplicate and are representative of two studies. Results are represented as oleic acid released (nmol/mg protein/h) from TGs (mean \pm SD; $n \geq 4$ /group). **B:** Mouse liver RNA from fasted LFD- and HFD-fed mice infected with either Ad-Luc or Ad-Elovl5 were prepared as described (14). mRNA levels of enzymes involved in TG hydrolysis (ATGL, PNPLA2; CGI58, ABHD5; ADPN, PNPLA3; TGH; and AADAC) were quantified by qRT-PCR (14). Expression of these transcripts is presented relative to the housekeeping gene cyclophilin. Results are presented as mRNA abundance fold change, relative to LFD Ad-Luc-infected mice; mean \pm SD, $n = 6$. **C–E:** Representative immunoblots, $n = 3$ mice per treatment and protein abundance of ATGL and CGI58 relative to loading control calnexin and Na,K-ATPase, respectively. Results were quantified and presented as protein abundance, relative to the loading control. Results are from two separate studies and expressed as mean \pm SD, $n = 6$. *a*, $P \leq 0.05$ versus Ad-Luc-infected mice fed the LFD (diet effect); *b*, $P \leq 0.05$ versus Ad-Luc-infected mice fed the LFD or HFD (genotype effect); *c*, $P \leq 0.05$ versus Ad-Elovl5-infected mice fed the LFD or HFD (diet-genotype interaction); two-way ANOVA with post hoc HSD test.

all PPAR subtypes are expressed in liver (54, 55) (supplementary Fig. III). As such, changes in Elovl5 activity can potentially impact PPAR signaling. We assessed the effects of diet and Elovl5 activity on hepatic gene expression by quantifying expression levels of several PPAR-regulated genes involved in hepatic lipid synthesis (14, 18, 54, 56) (Fig. 7).

Expression of enzymes involved in MUFA synthesis [Elovl6 and stearoyl-CoA desaturase 1 (SCD1)], PUFA synthesis [Elovl2, FA desaturase 1 (FADS1), and FA desaturase 2 (FADS2)], microsomal FAO (CYP4A10), hydrolysis of fatty acyl-CoA thioester formation [acyl CoA thioesterase 1 (ACOT1), cytosolic thioesterase 1 (CTE1) and hydroxyacyl-coenzyme A dehydrogenase/2-ketoacyl-coenzyme A thioesterase/enoyl-coenzyme A hydratase (trifunctional) protein (HADHA)], and synthesis of ketone bodies (HMG-CoASyn2), as well as the transcriptional coactivator peroxisome proliferator activated receptor-gamma co-activator 1 alpha (PGC1 α), were significantly suppressed by the HFD and elevated Elovl5 activity (Fig. 7A). In some cases, there was a significant diet-gene interaction (Elovl2, Fads2, CYP4A10, ACOT1, CTE1, and Hadha). In contrast, fibroblast growth factor 21 (FGF21) expression was not affected by diet but was induced by elevated Elovl5 activity only in HFD-med mice. PPAR γ expression was induced by the HFD but not affected by changes in Elovl5 activity. Induction of PPAR γ 2 mRNA is associated with hepatosteatosis in mice (57). Transcripts not significantly affected include PGC1 β , liver X receptor (LXR) α , and cytochrome P450 7alpha

hydroxylase (CYP7A). LXR ligands repress FGF21 (58); we see no evidence of HFD or Elovl5 repression of FGF21 expression.

Both elevated Elovl5 activity and the HFD induced PPAR α protein in hepatic nuclei (supplementary Fig. III). PPAR β / δ nuclear abundance was not affected by Elovl5, but PPAR γ 2 nuclear protein was suppressed by 50% in livers of obese mice expressing elevated Elovl5 activity. Effects of the HFD and Elovl5 activity on PPAR subtype nuclear abundance cannot explain the effects of diet and Elovl5 activity on PPAR-target gene expression (Fig. 7).

Diet and Elovl5 activity affect hepatic FA composition

Because Elovl5 plays a major role in both MUFA and PUFA metabolism and many of these FAs are PPAR ligands (Fig. 8A), we examined the effect of diet and Elovl5 on hepatic FAs. The HFD contains ample levels of 16:0, 18:0, 18:1,n-9, and 18:2,n-6; low levels of palmitoleic acid (16:1,n-7); and no detectable *cis*-VA (18:1,n-7) (14).

The ratio of product to precursor of hepatic FAs provides an indication of *in vivo* conversion. While the ratio of oleic acid (18:1,n-9) to stearate (18:0) was higher in HFD-fed mice, changes in this ratio were not found to be significant (Fig. 8B, C). *Cis*-VA is below detection in the HFD; as such, its presence in liver reflects its conversion from 16:1,n-7. Both 16:1,n-7 and 18:1,n-7 are lower in HFD-fed mice when compared with LFD-fed mice. Analysis of the 18:1,n-7/16:1,n-7 ratio reveals a significant increase in this ratio in mice infected with Ad-Elovl5, particularly in the

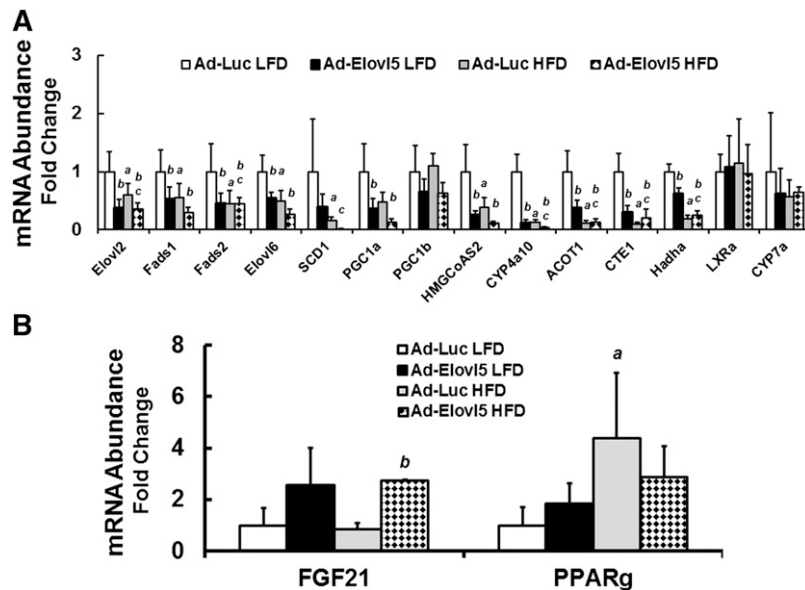


Fig. 7. Effect of diet and Elovl5 on the expression of genes involved in FA metabolism and oxidation. Hepatic mRNA extracted from LFD- and HFD-fed mice infected with either Ad-Luc or Ad-Elovl5 was used to quantify expression of specific transcripts by qRT-PCR (Materials and Methods). **A:** Hepatic abundance of transcripts suppressed by DIO, Elovl5 overexpression, or both. **B:** Hepatic abundance of transcripts induced by DIO, Elovl5 overexpression, or both. Results are from two separate studies and expressed as mean \pm SD, $n \geq 6$. *a*, $P \leq 0.05$ versus Ad-Luc-infected mice fed the LFD (diet effect); *b*, $P \leq 0.05$ versus Ad-Luc-infected mice fed the LFD or HFD (genotype effect); *c*, $P \leq 0.05$ versus Ad-Elovl5-infected mice fed the LFD (diet-genotype interaction); two-way ANOVA with post hoc HSD test.

HFD-fed mice, and reflects a significant diet-genotype interaction. Increased Elovl5 activity changes the type of MUFA synthesized in liver from n-9 MUFAs to n-7 MUFAs. This shift may have physiological relevance. In a comparative test, 50% more ^{14}C -18:1,n-7 was oxidized to ASM than ^{14}C -18:1,n-9 in AML12 mouse hepatocytes (supplementary Fig. IV). In this case, Elovl5 converts some FAs to a form that is more readily β -oxidized.

The HFD and Ad-Elovl5 infection also significantly affected hepatic PUFA content (Fig. 8D–G). This effect is most apparent in the sum (Σ) of C_{22} FAs and the ratio of n-3 PUFAs to n-6 PUFAs (Fig. 8D, E). Diet and Elovl5 activity had no effect on the sum of C_{20-22} n-6 PUFAs. Significant effects were seen in the increase in C_{22} n-3 PUFAs in livers of HFD-fed mice infected with Ad-Elovl5. These effects are seen in individual FAs and precursor-product analyses (Fig. 8F–I). Particularly relevant is the increased formation of intermediates in the n-6 PUFA pathway in mice infected with Ad-Elovl5 (Fig. 8F,G). In this group, ARA (20:4,n-6) is lower in obese mice than lean mice and is not restored with elevated Elovl5. One explanation is that Elovl5 converts 20:4,n-6 to 22:4,n-6 and 22:5,n-6 (Fig. 8G). Linoleic acid and ARA are the most common n-6 PUFAs accumulating in tissues. These PUFAs play a major role in membrane structure and cell signaling. Effects of C_{22} n-6 PUFAs on cell function, however, are not well studied.

Similar effects of Ad-Elovl5 infection are seen in the formation of C_{20-22} n-3 PUFAs (Fig. 8G–I). In this case, however, the process leads to the increased formation of 22:6,n-3, the major n-3 PUFA accumulating in tissues. Note that obesity is associated with a decline in the conversion of 18:3,n-3 to 22:6,n-3, and this is reversed by increased Elovl5 activity (Fig. 8J).

Exogenous FAs regulate PDK4 and ATGL abundance in HepG2 cells

To understand the impact of HFD- and Elovl5-induced changes in FAs on hepatic gene expression, we treated HepG2 cells with MUFAs and PUFAs (100 μM for 48 h) and quantified ATGL, CGI58, and PDK4 mRNA abundance (Fig. 9). PDK4 was used as a control for an established PPAR-target gene (48). PDK4 mRNA was significantly induced (0.5- to 5.5-fold) by several C_{20-22} n-3 and n-6 PUFAs, but no C_{18} MUFAs or 18:3,n-3. ATGL mRNA was induced $\sim 50\%$ by 18:1,n-7, 20:2,n-6, 20:4,n-6, 20:5,n-3, and 22:6,n-3. CGI58 mRNA was not significantly affected by any FAs.

PPARs regulate PDK4 and ATGL in HepG2 cells

To assess the role that PPAR subtypes played in the control of PDK4 and ATGL, we used selective PPAR agonists and antagonists and human HepG2 cells. Selective agonists for PPAR α (WY14643), PPAR β (GW0742), and PPAR γ (pioglitazone) induced PDK4 mRNA ≥ 15 -fold, and the PPAR-selective antagonists (GW6471, GSK3787, and T0070907) attenuated this response. Of the PPAR agonist examined, only the PPAR β -selective agonist (GW0742) significantly induced ATGL; the PPAR β -selective antagonist (GSK3787) attenuated this response. Interestingly, PPAR α and PPAR γ selective antagonists also suppressed ATGL mRNA below levels seen in cells treated with no agonist or antagonist. This outcome suggests that these selective antagonists may affect other factors controlling ATGL expression that are not involved in controlling PDK4 expression.

EPA is a well-established PPAR ligand. DHA, in contrast, is a weak PPAR agonist when compared with EPA. DHA, however, is retroconverted to EPA in hepatocytes and in

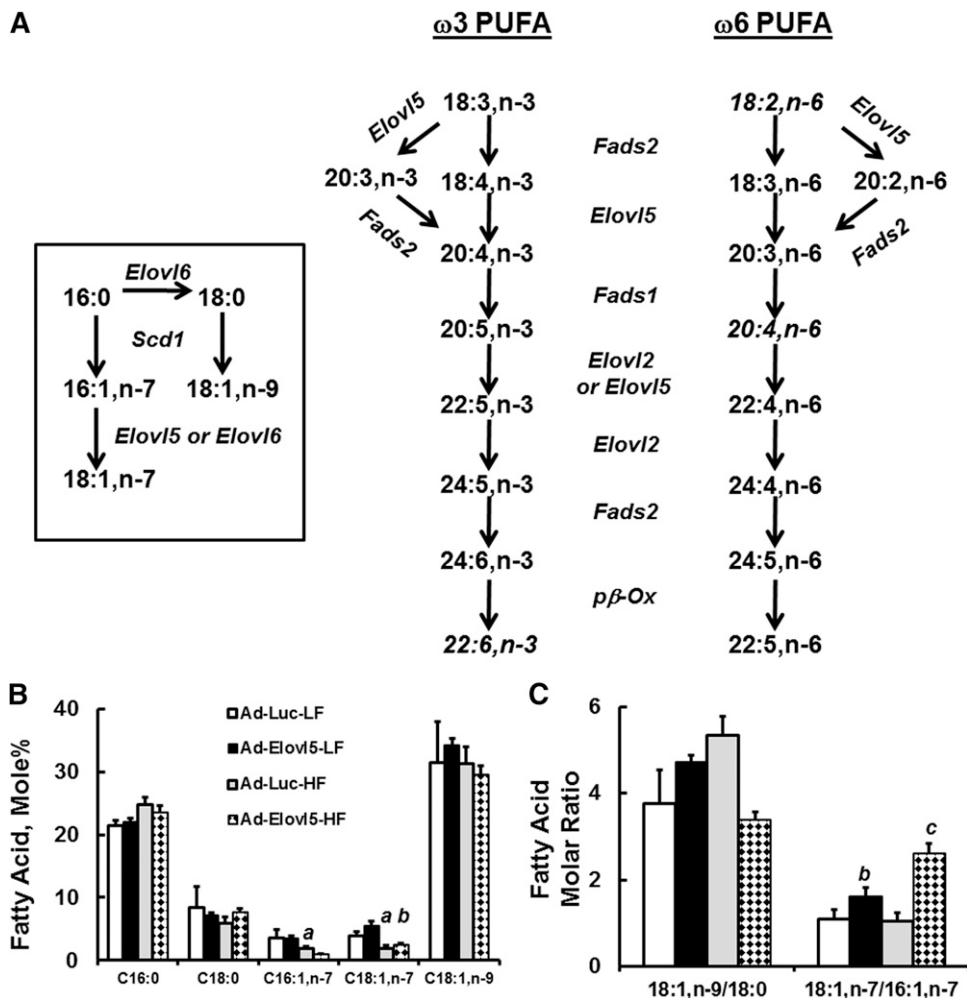


Fig. 8. Elevated hepatic Elovl5 activity changes hepatic MUFA and PUFA content. **A:** Pathways showing involvement of Elovl5 in MUFA and PUFA synthesis. **B:** Effect of diet and Elovl5 on hepatic saturated (SFA) and MUFA content. Results are expressed as mole %, mean \pm SD, $n = 4$. **C:** Mole ratio of 18:1,n-9 to 18:0 and 18:1,n-7 to 16:7,n-7. **D:** Sum of C_{20} and C_{22} FAs in livers of LFD- and HFD-fed mice infected with Ad-Luc or Ad-Elovl5. Results are given as the sum of the mole % of 20- or 22-carbon FAs. **E:** The ratio of the sum of all n-3 PUFAs to the sum of all n-6 PUFAs in livers of LFD- and HFD-fed mice infected with either Ad-Luc or Ad-Elovl5. **F:** Diet and Elovl5 effects on the mole % of 18:2,n-6 and 20:4,n-6. Inset: Mole ratio of 20:4,n-6 to 18:2,n-6. **G:** Diet and Elovl5 effects on the mole % of 18:3,n-6, 20:3,n-6, 22:4,n-6, and 22:5,n-6. **H:** Diet and Elovl5 effects on the mole % of 18:3,n-3, 20:5,n-3, 22:5,n-3, and 22:6,n-3. **I:** Mole ratio of 20:4,n-6 to 18:2,n-6; 20:5,n-3 to 18:3,n-3; and 22:5,n-3 to 18:3,n-3. **J:** Mole ratio of 22:6,n-3 to 18:3,n-3. All results are the mean \pm SD, $n \geq 4$ /group. *a*, $P \leq 0.05$ versus Ad-Luc-infected mice fed the LFD (diet effect); *b*, $P \leq 0.05$ versus Ad-Luc-infected mice fed the LFD or HFD (genotype effect); *c*, $P \leq 0.05$ versus Ad-Elovl5-infected mice fed the LFD (diet-genotype interaction); two-way ANOVA with post hoc HSD test.

vivo, making it difficult to determine whether DHA is a PPAR ligand (29). Nevertheless, we assessed the impact of the selective PPAR antagonists on EPA and DHA regulation of PDK4 and ATGL (**Fig. 10C, D**). EPA and DHA induced PDK4 by 14- and 9-fold, respectively. This response was significantly attenuated by all selective antagonists; GW6741 and GSK3787 were more effective than the PPAR γ antagonist (T0070907) at attenuating the induction of PDK4 by EPA and DHA. EPA and DHA induced ATGL mRNA by $\sim 70\%$, and this response was blocked by GSK3787, the PPAR β -selective antagonist (**Fig. 10C, D**). These findings indicate that PDK4 expression is highly responsive to PPAR agonist; this response is not selective to

specific PPAR subtypes. ATGL, in contrast, is weakly induced by the PPAR β agonist (GW0742). GW0742, EPA, and DHA induced ATGL mRNA to a similar level ($\sim 70\%$); this response was blocked by the PPAR β antagonist (GSK3787).

To assess the effects of PPAR β agonist (GW0742) on ATGL expression and lipid metabolism, AML12 cells were treated with vehicle (ethanol) or GW0742 for 48 h (**Fig. 11**). GW0742 induced ATGL $\sim 50\%$, which is similar to the induction of ATGL in HepG2 cells treated with GW0742, EPA, or DHA. Vehicle-, GW0742-, and GW0742 + GSK3787-treated AML12 cells received ^{14}C -18:2,n-6 for 6 h, and ^{14}C in TGs, polar lipids, and ASM was measured. GW0742-treated

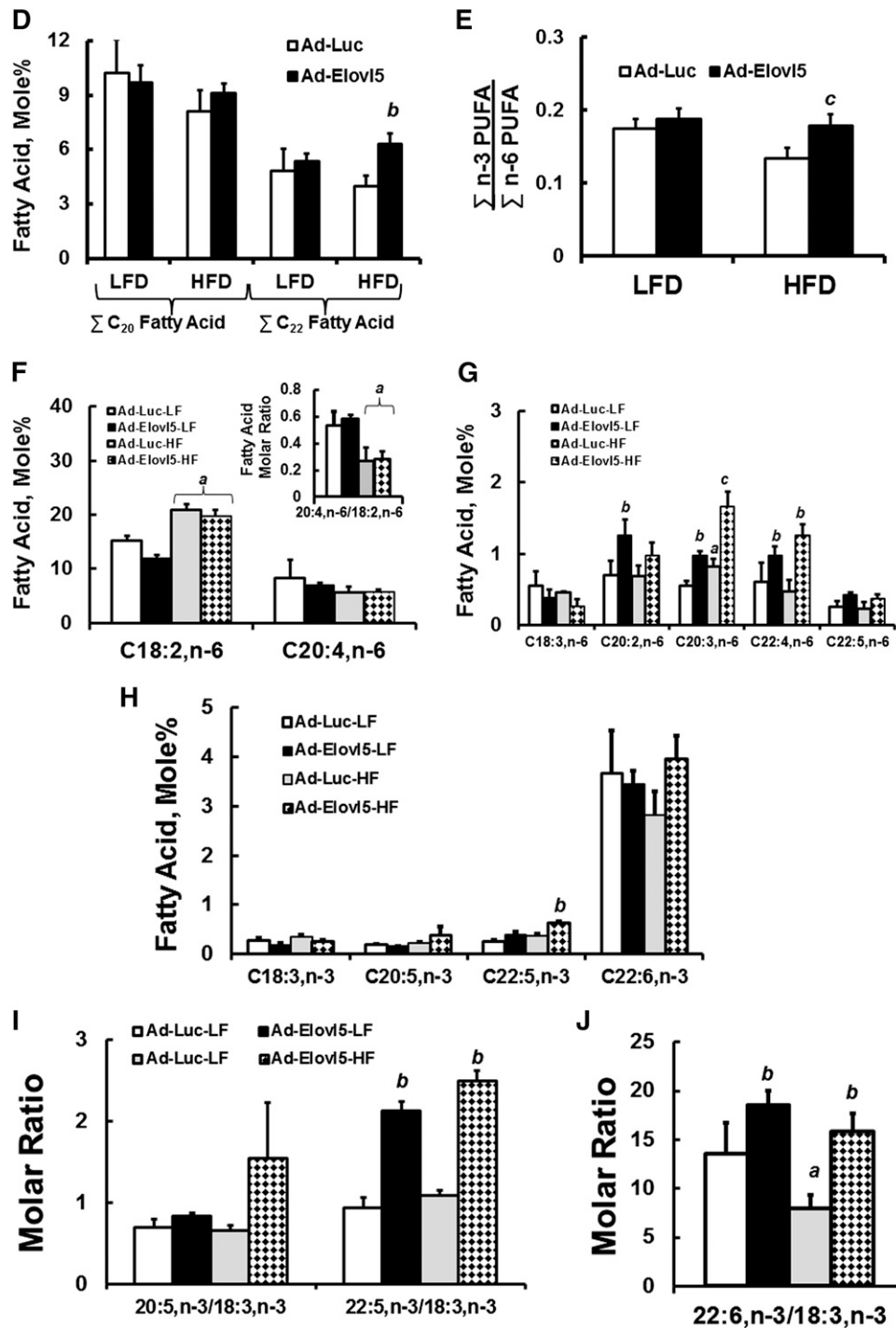


Fig. 8. Continued.

AML12 cells had ~25% lower ¹⁴C-18:2,n-6 in the TG fraction, while GW0742 + GSK3787 treatment reversed this effect. There was no change in the distribution of ¹⁴C in the polar lipids or ASM. Thus, PPAR β regulates ATGL expression and TG metabolism in AML12 cells.

We examined the time course for GW0742, EPA, and *cis*-VA regulation of PDK4 and ATGL in HepG2 cells (supplementary Fig. V, A–D). Both EPA and GW0742 induced a rapid and sustained (up to 48 h) increase in PDK4 and ATGL mRNA. *Cis*-VA induces rictor mRNA and protein in HepG2 cells (19). While *cis*-VA does not regulate PDK4

mRNA abundance, *cis*-VA induced ATGL in HepG2 cells. The response of ATGL to *cis*-VA treatment was slow when compared with rictor (supplementary Fig. V, C). Moreover, *cis*-VA induction of ATGL was not responsive to selective PPAR antagonist cotreatment. Thus, *cis*-VA regulation of ATGL is mediated by PPAR-independent mechanisms.

Influence of ATGL expression of PPAR signaling

Cellular levels of ATGL have been associated with changes in PPAR signaling (51–53, 59). PPAR activity is sensitive to changes in intracellular FA composition, particularly

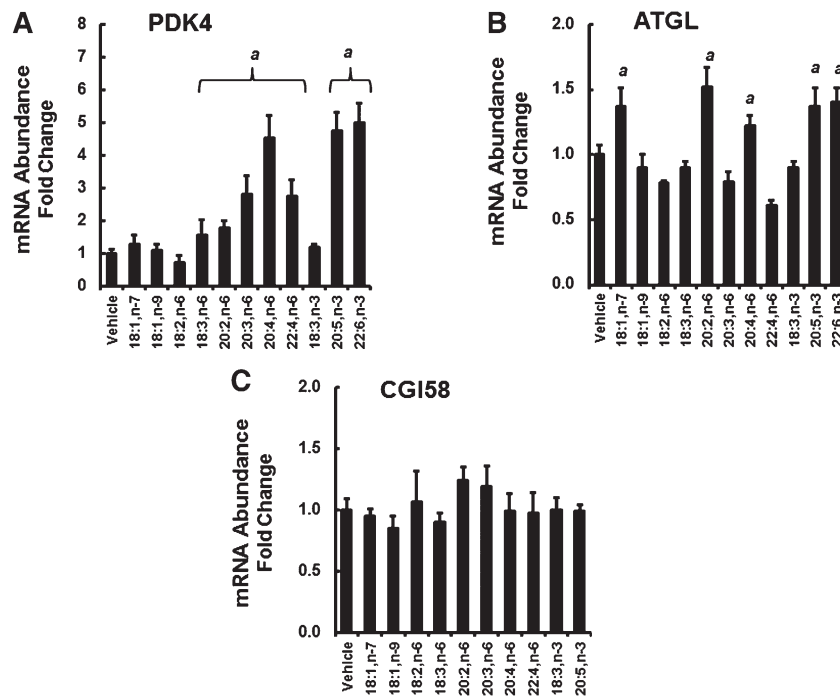


Fig. 9. FA effects on PDK4, ATGL, and CGI58 mRNA abundance in HepG2 cells. HepG2 cells were grown to 90% confluence in DMEM + high glucose and 10% fetal calf serum. Cells were serum-starved overnight and treated with 100 μ M FAs plus 33 micromolar BSA for 48 h. Cells were harvested and assayed for PDK4 (A), ATGL (B), CGI58 (C), and cyclophilin mRNA (Materials and Methods). Results are presented as mRNA abundance fold change, relative to vehicle-treated (ethanol, 0.1%) cells. Results are expressed as mean \pm SD, $n = 3$ and are representative of at least three separate studies. Comparisons between vehicle- and FA-treated cells were made by Student's *t*-test: *a*, $P \leq 0.05$ versus vehicle.

as NEFA. When rat primary hepatocytes are challenged with EPA, hepatic levels of nonesterified EPA, but not oleic acid, parallel changes in expression of CYP4A, a PPAR-target gene (29). To determine whether changes in ATGL expression affect PPAR signaling, AML12 hepatocytes were infected with recombinant adenoviruses that induce (Ad-ATGL) or suppress (Ad-shRNA-ATGL) ATGL protein abundance (Fig. 12). Ad-shRNA-ATGL infection of AML12 cells lowered ATGL mRNA and protein abundance by $\geq 75\%$, while Ad-ATGL infection of AML12 significantly induced ATGL mRNA and protein abundance by >20 -fold.

These changes in ATGL expression affected lipid metabolism. Uninfected cells and cells infected with Ad-shRNA-scramble, Ad-shRNA-ATGL, or Ad-ATGL were treated with 14 C-18:2,n-6 for 6 h. Cells were harvested for total lipid extraction, and media were quantified for ASM (Fig. 12D). Total cellular lipids were fractionated by TLC to quantify 14 C assimilated into TGs, NEFAs, and polar lipids. The level of 14 C recovered in the TG and polar lipid fractions represented $>99\%$ of all 14 C on the TLC plates. As expected, knockdown of ATGL increased the assimilation of 14 C-18:2,n-6 into TGs, while induction of ATGL lowered 14 C in the TG fraction. There was no effect of altered ATGL expression on 14 C-18:2,n-6 assimilation into polar lipids or its appearance in media as ASM.

We next examined the response of PDK4 to MUFA and PUFA challenge in AML12 cells with attenuated

or overexpressed ATGL (Fig. 12E). In cells infected with Ad-shRNA-scramble, PDK4 mRNA was induced (~ 2.2 -fold) by DHA, while 18:1,n-9 and 18:3,n-3 had no significant effect on PDK4 mRNA. Induction (Ad-ATGL-infected cells) or knockdown (Ad-shRNA-ATGL-infected cells) of ATGL protein did not significantly affect the response of PDK4 mRNA to FA challenge. As such, changes in ATGL expression do not affect FA regulation of PDK4, a PPAR-regulated gene, in AML12 cells.

DISCUSSION

The goal of this study was to define the molecular and metabolic basis for Elov15 control of HTG content in obese C57BL/6J mice. HFD-induced obesity in mice is associated with glucose intolerance, insulin resistance, and fatty liver (14). Accompanying fatty liver are increased ER stress and major changes in FA metabolism and gene expression (Figs. 2, 3, 7). We focused on Elov15 because its expression and activity were suppressed by $\geq 50\%$ in livers of mice fed the HFD (14). Moreover, Elov15 is a key enzyme in the pathway for n-7 MUFA and n-3 and n-6 PUFA synthesis, and these FAs regulate cell function through multiple mechanisms (14, 15, 18, 19).

The key findings of this study are as follows: 1) The HFD increased HTG content and the nuclear content of two ER-stress markers (XBPI and ATF6 α) (Figs. 1, 2). Increasing

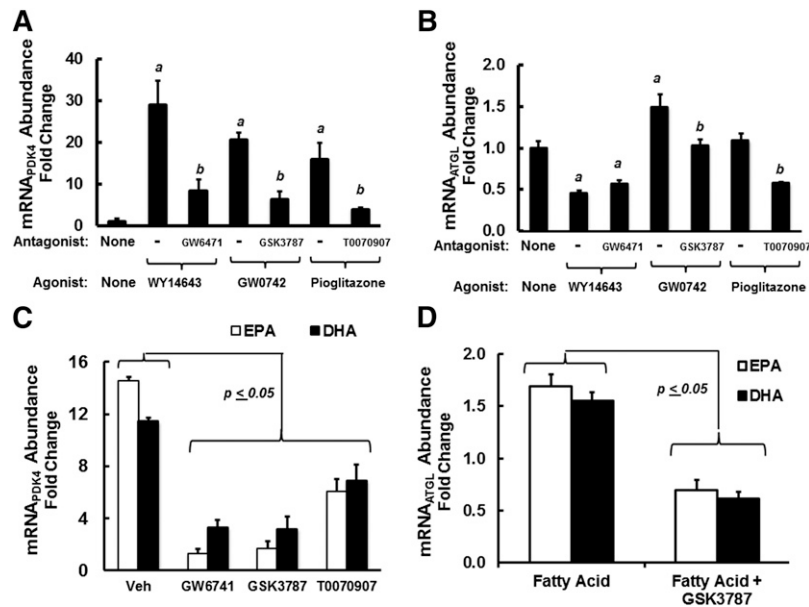


Fig. 10. Role of PPAR (α , β , and γ) in the FA regulation of PDK4 and ATGL in HepG2 cells. Preliminary dose response studies established the effective dose (ED_{50}) for induction and inhibition of PDK4 expression by PPAR agonists and antagonists, respectively. Using these concentrations, we assessed the PPAR agonist/antagonist effects on PDK4 and ATGL mRNA abundance in HepG2 cells. A and B: HepG2 cells were treated with PPAR α , PPAR β , and PPAR γ agonist at 10 μ M WY14643, 400 nM GW0742, and 1 μ M pioglitazone, respectively. Each group was also treated with the following PPAR antagonists (the PPAR antagonist concentration used was 4 \times the 50% inhibitory dose defined in preliminary studies): PPAR α antagonist, GW6471 (1 μ M); PPAR β antagonist, GSK3787 (1 μ M); and PPAR γ antagonist, T0070907 (4 nM). Cells were treated with agonist without and with antagonist for 48 h. Results are presented as mRNA abundance fold change for PDK4 (A) and ATGL (B); mean \pm SD, $n = 3$, $P \leq 0.05$, PPAR agonist versus no treatment; b , $P < 0.05$, PPAR antagonist versus PPAR agonist; Student's t -test. C and D: HepG2 cells were treated with EPA or DHA at 100 μ M in the absence or presence of PPAR α antagonist, GW6471 (1 μ M); PPAR β antagonist, GSK3787 (1 μ M); or PPAR γ antagonist, T0070907 (4 nM). As above, cells were harvested 48 h later for RNA extraction and quantitation of PDK4 (C), ATGL (D), and cyclophilin. Results are expressed as mRNA abundance fold change from cells treated with no FA; mean \pm SD, $n = 3$. The comparison is between FA-treated cells versus FA + PPAR selective antagonist-treated cells; Student's t -test.

Elovl5 activity in livers of obese mice lowered HTG and ER-stress markers. 2) Elevated Elovl5 activity increased TG catabolism in both lean and obese mice. FAO was low in livers of obese mice, and elevated Elovl5 did not increase the capacity for β -oxidation (Figs. 3–5). 3) Elovl5 effects on TG catabolism were associated with the induction of hepatic ATGL and CGI58 (Fig. 6), key proteins involved in HTG catabolism in several tissues, including liver (5, 52, 60, 61). 4) The HFD significantly altered hepatic n-7 MUFA and n-6 and n-3 PUFA content, and increased hepatic Elovl5 activity reversed many of these effects (Fig. 8). 5) Products of Elovl5 (i.e., EPA and DHA) induced ATGL, but not CGI58, expression in HepG2 cells through a PPAR β -dependent mechanism (Fig. 10). 6) The effects of the PPAR β -specific agonist, GW0742, on ATGL expression and TG metabolism in AML12 cells mimicked Elovl5 effects on ATGL and TG metabolism in liver (Fig. 10). These studies establish that Elovl5 activity regulates hepatic levels of FAs controlling PPAR β activity, ATGL, and TG catabolism.

TG metabolism

The effects of Elovl5 on TG catabolism reported here are consistent with the effects of Elovl5 knockdown on

hepatic lipid metabolism. Global knockout of Elovl5 in mice promotes fatty liver (10). This effect was attributed to the induction of sterol-regulatory element binding protein 1 (SREBP1) nuclear abundance and increased DNL. Products of Elovl5 (i.e., long-chain PUFAs) suppress hepatic SREBP1 nuclear abundance and DNL through multiple mechanisms (54). In HFD-induced obese mice, hepatic SREBP1 nuclear content is severely reduced (14); this reduction is linked to the significant reduction in mTORC1 (19), a key regulator of SREBP1 (62). As such, changes in SREBP1 and DNL and the lack of major effects on the GPAT1 fast-refeeding response (supplementary Fig. 1) cannot fully explain the accumulation of HTG in this model of HFD-induced fatty liver. The HFD does not decrease TG catabolism; the HFD attenuates ATGL, but not CGI58, protein abundance (Fig. 6). Increasing Elovl5 activity partially restored hepatic ATGL, while significantly increasing hepatic CGI58 protein content (Fig. 6C–E). These events are associated with increased capacity for TG catabolism in hepatic extracts (Fig. 6A, B). As such, Elovl5 activity controls TG metabolism by regulating both TG production (10) and TG catabolism (Fig. 6).

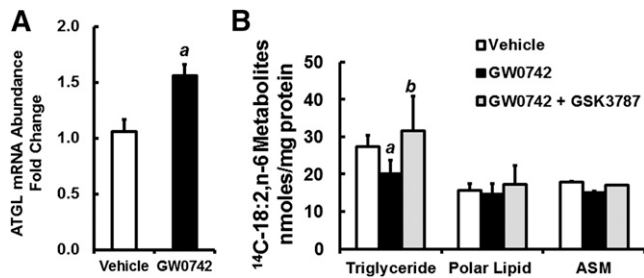


Fig. 11. Effect of PPAR β agonist and antagonist on ATGL expression and lipid metabolism in AML12 cells. A: AML12 cells at \sim 80% confluence were treated with vehicle (0.1% ethanol) or GW0742 (400 nM) for 48 h. RNA was isolated to measure ATGL and cyclophilin. Results are expressed as ATGL mRNA abundance fold change; mean \pm SD, $n = 4$. *a*, $P < 0.05$ versus vehicle-treated cells. B: AML12 cells were treated with vehicle, GW0742 (400 nM), or GW0742 (400 nM) + GSK3787 (1 μ M) for 48 h. Cells were treated with 100 μ M 14 C-18:2,n-6 for 6 h in serum-free DMEM/F12 medium containing BSA (33 μ M). After FA treatment, cells were recovered for total protein measurement and total lipid extraction. Media was recovered for the measurement of FAO as ASM as described (22). Total lipids were separated by TLC, and the distribution of 14 C in various lipids was quantified by phosphorimage analysis as described (22). Results are represented as 14 C-18:2,n-6 metabolites (as TGs, polar lipids, or ASM), nanomoles per milligram of protein; mean \pm SD, $n = 4$. *a*, $P < 0.05$ versus vehicle-treated cells; *b*, $P < 0.05$ versus GW0742-treated cells; Student's *t*-test.

FAO

Hepatic FAO was examined at multiple levels. Finding that the HFD lowered blood levels of β -hydroxybutyrate and hepatic capacity for β -oxidation (Figs. 1, 3) was consistent with the known effects of the HFD on hepatic FAO (25). The restoration of plasma β -hydroxybutyrate in obese mice with elevated Elov15 activity suggested improved β -oxidation (Fig. 1B). This outcome, however, was misleading because a measure of the capacity for β -oxidation in liver extracts (Fig. 3A) established that the HFD lowered hepatic β -oxidation by 50%, and elevated Elov15 activity did not restore β -oxidation to levels seen in lean mice. Finding increased levels of hepatic fatty acyl carnitines in HFD-fed obese mice with elevated Elov15 activity suggested that mitochondrial β -oxidation was intact but may have been insufficient to deal with the excessive NEFA entering liver from TG catabolism. Acyl carnitines accumulate in tissues and blood level of individuals with in-born errors in FAO (63). Our studies identified a broad spectrum of hepatic acyl carnitines (Fig. 5) and suggest that the defect in FAO was not localized to a specific enzyme.

The low capacity for mitochondrial FAO in livers of obese mice has been linked to SIRT3 activity and the acetylation status of specific mitochondrial proteins (e.g., LCAD) (25). While we did not examine mitochondrial protein acetylation, we did examine the effect of the HFD and Elov15 on expression of SIRT3 and enzymes involved in β -oxidation. The HFD did not attenuate the mRNAs encoding these proteins. Increasing hepatic Elov15 in livers of obese mice, however, induced mRNAs encoding CPT2, LCAD, and MCAD modestly (i.e., \sim 2-fold), but not SIRT3

(Fig. 3). Despite the Elov15 effects on the expression of these enzymes, FAO was not increased. Increased Elov15 activity also suppressed PDK4 protein abundance by \sim 50% in both lean and obese mice (Fig. 4). This change in PDK4 had no effect on the phosphorylation of the PDE1 α , a key pyruvate dehydrogenase regulatory subunit (48). Together, these findings indicate that increasing Elov15 activity does not increase hepatic capacity for β -oxidation. This outcome agrees with a previous study showing that increasing Elov15 activity in HepG2 cells had no significant effect on FAO (22).

Unsaturated FA metabolism and gene expression

Both the HFD and changes in Elov15 activity were associated with significant effects on hepatic MUFA and PUFA content (Fig. 8). The HFD decreased hepatic DHA content, while increasing Elov15 activity reversed this effect. Western diet-induced fatty liver in *Ldlr*^{-/-} mice is also associated with lower hepatic DHA content (12). Increasing Elov15 activity in livers of obese mice also increased 18:1,n-7, 22:4,n-6, and 22:5,n-6 when compared with their precursors. Testing these and other FAs in HepG2 cells established that ATGL mRNA, but not CGI58 mRNA, was modestly (\geq 50%) induced by 18:1,n-7 and several C₂₀₋₂₂ n-3 and n-6 PUFAs, but not oleic acid (18:1,n-9) or C₁₈ PUFAs (Fig. 9).

PUFAs regulate multiple pathways controlling gene expression and cell signaling (54). Elov15 is a PPAR-target gene, and its activity controls cellular levels of putative PPAR ligands (15) (Fig. 8A). The HFD significantly attenuated the expression of multiple PPAR-target genes (Fig. 7). One explanation for the HFD effect on PPAR signaling is that the HFD significantly enriches the liver with SFAs and MUFAs, particularly 18:1,n-9. In rat primary hepatocytes, 18:1,n-9 does not activate PPAR α (29). The HFD also suppressed the expression of genes involved in unsaturated FA synthesis (Elov12, Fads1, Elov16, and SCD1). Fads1, Elov16, and SCD1 are regulated by PPAR and SREBP1 (15, 54). As noted previously, SREBP1 is knocked down by the HFD. Of the genes knocked down by the HFD, none were induced by elevated Elov15 activity.

Another explanation for the lack of induction of these genes is the formation of C₂₂ PUFAs in response to elevated Elov15 activity. Our previous studies with rat primary hepatocytes suggested that C₂₂ n-3 PUFAs were poor activators of PPAR (29). As such, the increased hepatic abundance of C₂₂ n-3 and n-6 PUFAs may fail to activate PPAR or interfere with other regulators of PPAR signaling. It remains unclear if C₂₂ n-3 and n-6 PUFAs are PPAR ligands. DHA activates PPAR because it is retroconverted to EPA, and EPA is a well-established PPAR ligand. Because PUFAs also regulate multiple signaling pathways originating from the plasma membrane (54), it is also possible that C₂₂ PUFA-regulated cell signaling pathways affect PPAR function. More study is required to resolve this issue.

PPAR signaling

PDK4 was used as a model PPAR-target gene (48). Its expression in HepG2 cells is induced by selective PPAR

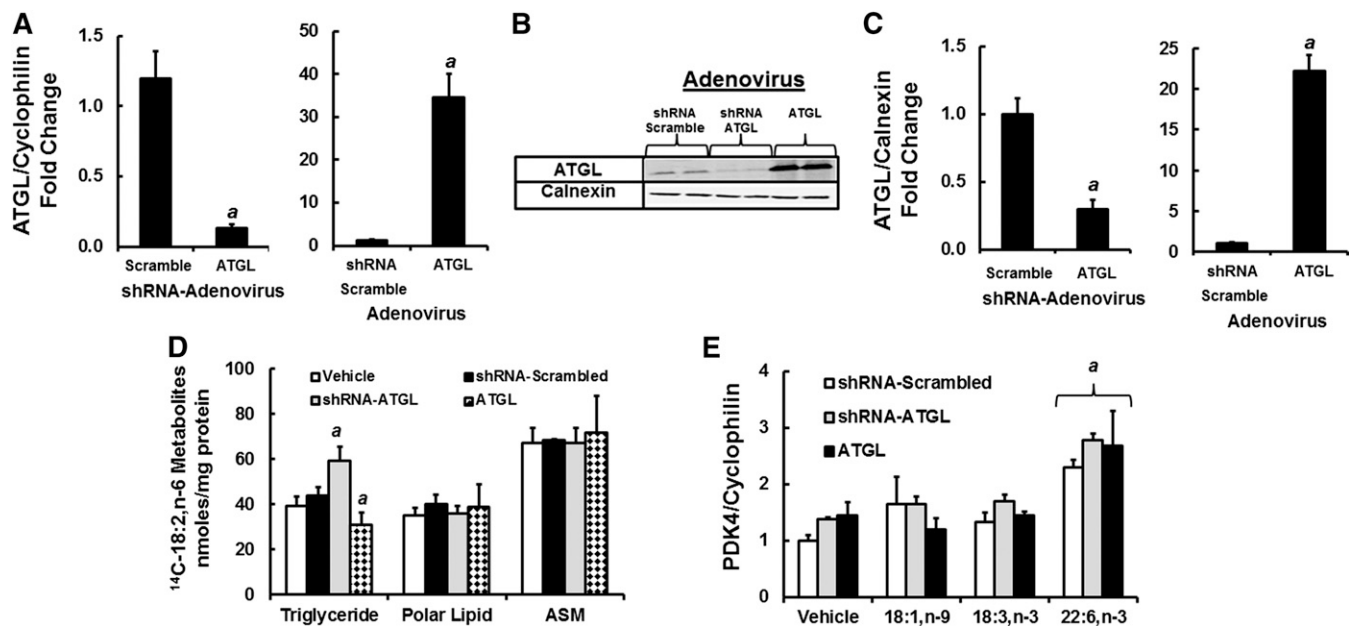


Fig. 12. Effect of over- and underexpression of ATGL on ^{14}C -18:2,n-6 metabolism and PDK4 expression in AML12 cells. AML12 cells at $\sim 80\%$ confluence were infected with Ad-shRNA scrambled, Ad-shRNA-ATGL, or Ad-ATGL at 40 IU/cell. Levels of ATGL expression were assessed by mRNA (A) and protein (B and C) measurements. The loading control for the immunoblots was calnexin. Results are the mean \pm SD, $n = 4$. *a*, $P < 0.05$ versus Ad-shRNA-scrambled-infected cells. D: AML12 cells not infected or infected with Ad-shRNA-scrambled, Ad-shRNA-ATGL, or Ad-ATGL as described previously were treated with ^{14}C -18:2,n-6 (100 μM) in serum-free media containing BSA (33 μM) as described in Fig. 11. Six hours later, cells were harvested for protein measurement and total lipids (organic extraction). The media was assayed for ASM, and the total lipid extract was separated by TLC. The distribution of ^{14}C -18:2,n-6 metabolites was quantified as described in Fig. 11. E: AML 12 cells infected with Ad-shRNA-scrambled, Ad-shRNA-ATGL, or Ad-ATGL as described previously were treated with vehicle or FAs (18:1,n-9, 18:3,n-3, or 22:6,n-3) at 100 μM (plus 33 μM BSA) for 48 h and then extracted for RNA to measure PDK4 and cyclophilin expression. Results in D and E are representative of ≥ 3 separate experiments in duplicate; mean \pm SD, $n = 3$. *a*, $P < 0.05$ versus vehicle or Ad-shRNA-scrambled-infected cells; Student's *t*-test.

agonists and repressed by selective PPAR antagonists (Fig. 10). EPA and DHA induction of PDK4 is blocked by all PPAR antagonists. ATGL, in contrast, was only induced by the PPAR β selective agonist (GW0742). EPA and DHA induction of ATGL was attenuated by the selective PPAR β antagonist, GSK3787. Further examination established that treatment of AML12 cells with GW0742 increased ATGL mRNA $\sim 50\%$ and lowered the incorporation of ^{14}C -18:2,n-6 into TGs by 25%. FAO, however, was not affected by GW0742 (Fig. 11). Thus, EPA and DHA regulate ATGL expression in human (HepG2) and mouse (AML12) cells through a PPAR β -dependent mechanism.

Cis-VA, the MUFA product of Elovl5 elongation of palmitoleic acid, induced ATGL, but not PDK4 (Fig. 9). The time course for this induction was slow when compared with *cis*-VA induction of rictor (19) (supplementary Fig. IV). *Cis*-VA induction of ATGL was not attenuated by any selective PPAR antagonist. Moreover, the combination of GW0742 and *cis*-VA acid did not yield an additive response. Thus, PPAR signaling is not required for *cis*-VA induction of ATGL.

In adipocytes, ATGL expression is repressed by insulin, at least in part through mTORC1 (64), and induced in fasting in response to FoxO1 binding to the ATGL promoter (65). The HFD promotes hyperglycemia, in part by inducing hepatic GNG, an effect that is mediated by increased nuclear

abundance of FoxO1 and the induction of phosphoenolpyruvate carboxykinase and glucose-6 phosphatase. Elevated hepatic Elovl5 activity suppresses expression of genes involved in GNG by increasing FoxO1 phosphorylation and lowering FoxO1 nuclear content. The mechanism linking these events involves increased hepatic content of *cis*-VA, which induces rictor and activates the mTORC2-AKT2 pathway in livers of fasting mice (19). *Cis*-VA regulation of FoxO1 is inconsistent with the induction of ATGL in livers of fasted mice. An alternative pathway might involve mTORC1. The HFD suppresses hepatic raptor expression leading to a significant decline in mTORC1 signaling (i.e., p70S6kinase³⁸⁹-T) (19). Elevated Elovl5 activity suppresses mTORC1 further. As such, *cis*-VA may relieve mTORC1 inhibition of ATGL by downregulating mTORC1. Future studies will be required to test this hypothesis.

Finally, cellular ATGL levels have been linked to PPAR signaling (51–53, 59). Some have suggested that ATGL regulates cellular levels of FAs controlling PPAR activity. We examined the effect of altered ATGL expression on PDK4 signaling in mouse AML12 hepatocytes and used an adenoviral approach to knockdown (Ad-shRNA-ATGL) or overexpress ATGL (Ad-ATGL). As expected, these treatments had major effects on AML12 cell ATGL mRNA and protein (Fig. 12A–C), as well as the amount of ^{14}C -18:2,n-6 recovered in the TG fraction (Fig. 12D). Challenging


AML12 cells with 18:1,n-9, 18:3,n-3, and 22:6,n-3 (DHA) established that only DHA induced PDK4 mRNA (2.5-fold) (Fig. 12E). This response was not influenced by major changes in ATGL protein abundance (Fig. 12A–C). The response of PDK4 to FA challenge was governed by the type of FA used to activate PPAR and not the level of ATGL expression. This result is consistent with our previous studies in rat primary hepatocytes (29).

This outcome does not agree with the reports of others (52, 59) and may reflect differences in cell culture models, methods of PPAR activation, or the type of FAs stored as neutral lipid in cells. In this regard, the HFD knocks down the expression of multiple PPAR target genes (Fig. 7) including Elov15 and ATGL. We suspect this outcome may be linked to the enrichment of the fatty liver with SFAs and MUFAs and its depletion of C_{20–22} PUFAs (Fig. 8). Moreover, C₁₈ MUFAs and PUFAs do not induce PDK4, a PPAR-target gene (Fig. 9), and C₁₈ MUFAs do not activate PPAR α in rat primary hepatocytes (29). The capacity of ATGL to regulate PPAR-target genes may depend on the level of C_{20–22} PUFAs stored in TGs.

Unanswered questions

A key unanswered question is how a change in Elov15 activity in vivo regulates CGI58 protein abundance. According to Badin et al. (66), in skeletal muscle of HFD-fed mice, CGI58 is induced, while ATGL expression is repressed. These authors report significant changes in skeletal muscle DAG and membrane translocation of protein kinase C subtypes (PKC- θ and PKC- ϵ). As such, future studies will examine the role that PKCs and other signaling mechanisms play in Elov15 control of CGI58 expression. Finally, our studies revealed a suppressive effect of elevated Elov15 activity on TGH, also known as CES3 (Fig. 6). The liver expresses other CES subtypes (e.g., CES1) and possibly other enzymes involved in neutral lipid catabolism. Future studies will need to assess the impact of diet and PUFA metabolism on these enzymes.

Summary

We have established that increasing Elov15 activity in livers of obese mice induces ATGL and CGI58 protein. This effect is associated with increased HTG catabolism, hepatic acyl carnitines, and plasma β -hydroxybutyrate, but not increased capacity for β -oxidation. We also established that *cis*-VA, EPA, and DHA, products of Elov15 activity, induced hepatic ATGL, but not CGI58 expression. EPA and DHA, but not *cis*-VA, mediate control of ATGL through a PPAR β -dependent mechanism. As such, hepatic PUFA metabolism plays an important role in controlling hepatic TG catabolism through PPAR β -dependent mechanism regulation of ATGL expression. 

REFERENCES

1. Greenfield, V., O. Cheung, and A. J. Sanyal. 2008. Recent advances in nonalcoholic fatty liver disease. *Curr. Opin. Gastroenterol.* **24**: 320–327.
2. Rodríguez-Hernández, H., L. E. Simental-Mendía, G. Rodríguez-Ramírez, and M. A. Reyes-Romero. 2013. Obesity and inflammation:

epidemiology, risk factors, and markers of inflammation. *Int. J. Endocrinol.* **2013**: 678159.

3. McCullough, A. J. 2006. Pathophysiology of nonalcoholic steatohepatitis. *J. Clin. Gastroenterol.* **40** (Suppl. 1): S17–S29.
4. Quiroga, A. D., and R. Lehner. 2012. Liver triacylglycerol lipases. *Biochim. Biophys. Acta.* **1821**: 762–769.
5. Reid, B. N., G. P. Ables, O. A. Otlivanchik, G. Schoiswohl, R. Zechner, W. S. Blaner, I. J. Goldberg, R. F. Schwabe, S. C. Chua, Jr., and L. S. Huang. 2008. Hepatic overexpression of hormone-sensitive lipase and adipose triglyceride lipase promotes fatty acid oxidation, stimulates direct release of free fatty acids, and ameliorates steatosis. *J. Biol. Chem.* **283**: 13087–13099.
6. Depner, C. M., M. Torres-Gonzalez, S. Tripathy, G. Milne, and D. B. Jump. 2012. Menhaden oil decreases high-fat diet-induced markers of hepatic damage, steatosis, inflammation, and fibrosis in obese Ldlr $^{-/-}$ mice. *J. Nutr.* **142**: 1495–1503.
7. Qureshi, K., and G. A. Abrams. 2007. Metabolic liver disease of obesity and role of adipose tissue in the pathogenesis of nonalcoholic fatty liver disease. *World J. Gastroenterol.* **13**: 3540–3553.
8. Petit, J. M., B. Guiu, L. Duveillard, V. Jooste, M. C. Brindisi, A. Athias, B. Bouillet, M. Habchi, V. Cottet, P. Gambert, et al. 2012. Increased erythrocytes n-3 and n-6 polyunsaturated fatty acids is significantly associated with a lower prevalence of steatosis in patients with type 2 diabetes. *Clin. Nutr.* **31**: 520–525.
9. Matsuzaka, T., H. Shimano, N. Yahagi, T. Kato, A. Atsumi, T. Yamamoto, N. Inoue, M. Ishikawa, S. Okada, N. Ishigaki, et al. 2007. Crucial role of a long-chain fatty acid elongase, Elov16, in obesity-induced insulin resistance. *Nat. Med.* **13**: 1193–1202.
10. Moon, Y. A., R. E. Hammer, and J. D. Horton. 2009. Deletion of ELOVL5 leads to fatty liver through activation of SREBP-1c in mice. *J. Lipid Res.* **50**: 412–423.
11. Yang, Z. H., H. Miyahara, and A. Hatanaka. 2011. Chronic administration of palmitoleic acid reduces insulin resistance and hepatic lipid accumulation in KK-Ay mice with genetic type 2 diabetes. *Lipids Health Dis.* **10**: 120.
12. Depner, C. M., K. A. Philbrick, and D. B. Jump. 2013. Docosahexaenoic acid attenuates hepatic inflammation, oxidative stress, and fibrosis without decreasing hepatosteatosis in a Ldlr $^{-/-}$ mouse model of western diet-induced nonalcoholic steatohepatitis. *J. Nutr.* **143**: 315–323.
13. Guo, X., H. Li, H. Xu, V. Halim, W. Zhang, H. Wang, K. T. Ong, S-L. Woo, R. L. Walzem, D. G. Mashek, et al. 2012. Palmitoleate induces hepatic steatosis but suppresses liver inflammatory responses in mice. *PLoS One.* **7**: e39286.
14. Tripathy, S., M. Torres-Gonzalez, and D. B. Jump. 2010. Elevated hepatic fatty acid elongase-5 activity corrects dietary fat-induced hyperglycemia in obese C57BL/6J mice. *J. Lipid Res.* **51**: 2642–2654.
15. Wang, Y., D. Botolin, J. Xu, B. Christian, E. Mitchell, B. Jayaprakasam, M. G. Nair, J. M. Peters, J. V. Busik, L. K. Olson, et al. 2006. Regulation of hepatic fatty acid elongase and desaturase expression in diabetes and obesity. *J. Lipid Res.* **47**: 2028–2041. [Erratum. 2006. *J. Lipid Res.* **47**(10):2353.]
16. Green, C. D., C. G. Ozguden-Akkoc, Y. Wang, D. B. Jump, and L. K. Olson. 2010. Role of fatty acid elongases in determination of de novo synthesized monounsaturated fatty acid species. *J. Lipid Res.* **51**: 1871–1877.
17. Ohno, Y., S. Suto, M. Yamanaka, Y. Mizutani, S. Mitsutake, Y. Igarashi, T. Sassa, and A. Kihara. 2010. ELOVL1 production of C24 acyl-CoAs is linked to C24 sphingolipid synthesis. *Proc. Natl. Acad. Sci. USA.* **107**: 18439–18444.
18. Wang, Y., M. Torres-Gonzalez, S. Tripathy, D. Botolin, B. Christian, and D. B. Jump. 2008. Elevated hepatic fatty acid elongase-5 activity affects multiple pathways controlling hepatic lipid and carbohydrate composition. *J. Lipid Res.* **49**: 1538–1552.
19. Tripathy, S., and D. B. Jump. 2013. Elov15 regulates the mTORC2-Akt-FOXO1 pathway by controlling hepatic *cis*-vaccenic acid synthesis in diet-induced obese mice. *J. Lipid Res.* **54**: 71–84.
20. Lass, A., R. Zimmermann, G. Haemmerle, M. Riederer, G. Schoiswohl, M. Schweiger, P. Kienesberger, J. G. Strauss, G. Gorkiewicz, and R. Zechner. 2006. Adipose triglyceride lipase-mediated lipolysis of cellular fat stores is activated by CGI-58 and defective in Chanarin-Dorfman Syndrome. *Cell Metab.* **3**: 309–319.
21. Miyoshi, H., J. W. Perfield II, M. S. Obin, and A. S. Greenberg. 2008. Adipose triglyceride lipase regulates basal lipolysis and lipid droplet size in adipocytes. *J. Cell. Biochem.* **105**: 1430–1436.

22. Jump, D. B., M. Torres-Gonzalez, and L. K. Olson. 2011. Soraphen A, an inhibitor of acetyl CoA carboxylase activity, interferes with fatty acid elongation. *Biochem. Pharmacol.* **81**: 649–660.
23. Millington, D. S., and R. D. Stevens. 2011. Acylcarnitines: analysis in plasma and whole blood using tandem mass spectrometry. *Methods Mol. Biol.* **708**: 55–72.
24. Ferrara, C. T., P. Wang, E. C. Neto, R. D. Stevens, J. R. Bain, B. R. Wenner, O. R. Ilkayeva, M. P. Keller, D. A. Blasiolo, C. Kendziorski, et al. 2008. Genetic networks of liver metabolism revealed by integration of metabolic and transcriptional profiling. *PLoS Genet.* **4**: e1000034.
25. Hirschey, M. D., T. Shimazu, E. Goetzman, E. Jing, B. Schwer, D. B. Lombard, C. A. Grueter, C. Harris, S. Biddinger, O. R. Ilkayeva, et al. 2010. SIRT3 regulates mitochondrial fatty-acid oxidation by reversible enzyme deacetylation. *Nature.* **464**: 121–125.
26. Kim, J.-Y., R. C. Hickner, R. L. Cortright, G. L. Dohm, and J. A. Houmard. 2000. Lipid oxidation is reduced in obese human skeletal muscle. *Am. J. Physiol. Endocrinol. Metab.* **279**: E1039–E1044.
27. Schweiger, M., R. Schreiber, G. Haemmerle, A. Lass, C. Fledelius, P. Jacobsen, H. Tornqvist, R. Zechner, and R. Zimmermann. 2006. Adipose triglyceride lipase and hormone-sensitive lipase are the major enzymes in adipose tissue triacylglycerol catabolism. *J. Biol. Chem.* **281**: 40236–40241.
28. Alsted, T. J., L. Nybo, M. Schweiger, C. Fledelius, P. Jacobsen, R. Zimmermann, R. Zechner, and B. Kiens. 2009. Adipose triglyceride lipase in human skeletal muscle is upregulated by exercise training. *Am. J. Physiol. Endocrinol. Metab.* **296**: E445–E453.
29. Pawar, A., and D. B. Jump. 2003. Unsaturated fatty acid regulation of peroxisome proliferator-activated receptor alpha activity in rat primary hepatocytes. *J. Biol. Chem.* **278**: 35931–35939.
30. Depner, C. M., M. G. Traber, G. Bobe, K. M. Bohren, E. Morinkensicki, G. Milne, and D. B. Jump. 2013. A metabolomic analysis of omega-3 fatty acid mediated attenuation of western diet-induced non-alcoholic steatohepatitis in LDLR^{-/-} mice. *PLoS ONE.* **8**: e83756.
31. Pagliassotti, M. J. 2012. Endoplasmic reticulum stress in nonalcoholic fatty liver disease. *Annu. Rev. Nutr.* **32**: 17–33.
32. Ozcan, U., Q. Cao, E. Yilmaz, A. H. Lee, N. N. Iwakoshi, E. Ozdelen, G. Tuncman, C. Gorgun, L. H. Glimcher, and G. S. Hotamisligil. 2004. Endoplasmic reticulum stress links obesity, insulin action, and type 2 diabetes. *Science.* **306**: 457–461.
33. Violante, S., L. Ijlst, H. van Lenthe, I. T. de Almeida, R. J. Wanders, and F. V. Ventura. 2010. Carnitine palmitoyltransferase 2: new insights on the substrate specificity and implications for acylcarnitine profiling. *Biochim. Biophys. Acta.* **1802**: 728–732.
34. Ramsay, R. R., R. D. Gandour, and F. R. van der Leij. 2001. Molecular enzymology of carnitine transfer and transport. *Biochim. Biophys. Acta.* **1546**: 21–43.
35. Longo, N., C. Amat di San Filippo, and M. Pasquali. 2006. Disorders of carnitine transport and the carnitine cycle. *Am. J. Med. Genet. C Semin. Med. Genet.* **142C**: 77–85.
36. Attia, R. R., P. Sharma, R. C. Janssen, J. E. Friedman, X. Deng, J. S. Lee, M. B. Elam, G. A. Cook, and E. A. Park. 2011. Regulation of pyruvate dehydrogenase kinase 4 (PDK4) by CCAAT/enhancer-binding protein beta (C/EBPbeta). *J. Biol. Chem.* **286**: 23799–23807.
37. Hwang, B., P. Wu, and R. A. Harris. 2012. Additive effects of clofibrate and pyruvate dehydrogenase kinase isoenzyme 4 (PDK4) deficiency on hepatic steatosis in mice fed a high saturated fat diet. *FEBS J.* **279**: 1883–1893.
38. McCarty, M. F. 2005. High mitochondrial redox potential may promote induction and activation of UCP2 in hepatocytes during hepatothermic therapy. *Med. Hypotheses.* **64**: 1216–1219.
39. Bermejo-Nogales, A., L. Benedito-Palos, J. A. Caldich-Giner, and J. Perez-Sanchez. 2011. Feed restriction up-regulates uncoupling protein 3 (UCP3) gene expression in heart and red muscle tissues of gilthead sea bream (*Sparus aurata* L.) New insights in substrate oxidation and energy expenditure. *Comp. Biochem. Physiol. A Mol. Integr. Physiol.* **159**: 296–302.
40. Boudina, S., Y. H. Han, S. Pei, T. J. Tidwell, B. Henrie, J. Tuinei, C. Olsen, S. Sena, and E. D. Abel. 2012. UCP3 regulates cardiac efficiency and mitochondrial coupling in high fat-fed mice but not in leptin-deficient mice. *Diabetes.* **61**: 3260–3269.
41. Musa, C. V., A. Mancini, A. Alfieri, G. Labruna, G. Valerio, A. Franzese, F. Pasanisi, M. R. Licenziati, L. Sacchetti, and P. Buono. 2012. Four novel UCP3 gene variants associated with childhood obesity: effect on fatty acid oxidation and on prevention of triglyceride storage. *Int. J. Obes. (Lond.).* **36**: 207–217.
42. Senese, R., V. Valli, M. Moreno, A. Lombardi, R. A. Busiello, F. Cioffi, E. Silvestri, F. Goglia, A. Lanni, and P. de Lange. 2011. Uncoupling protein 3 expression levels influence insulin sensitivity, fatty acid oxidation, and related signaling pathways. *Pflügers Arch.* **461**: 153–164.
43. Cole, M. A., A. J. Murray, L. E. Cochlin, L. C. Heather, S. McAleese, N. S. Knight, E. Sutton, A. A. Jamil, N. Parassol, and K. Clarke. 2011. A high fat diet increases mitochondrial fatty acid oxidation and uncoupling to decrease efficiency in rat heart. *Basic Res. Cardiol.* **106**: 447–457.
44. Huang, J., D. Jones, B. Luo, M. Sanderson, J. Soto, E. D. Abel, R. C. Cooksey, and D. A. McClain. 2011. Iron overload and diabetes risk: a shift from glucose to fatty acid oxidation and increased hepatic glucose production in a mouse model of hereditary hemochromatosis. *Diabetes.* **60**: 80–87.
45. Koves, T. R., J. R. Ussher, R. C. Noland, D. Slentz, M. Mosedale, O. Ilkayeva, J. Bain, R. Stevens, J. R. Dyck, C. B. Newgard, et al. 2008. Mitochondrial overload and incomplete fatty acid oxidation contribute to skeletal muscle insulin resistance. *Cell Metab.* **7**: 45–56.
46. Islam, A., A. E. Civitarese, R. L. Hesslink, and D. D. Gallaheer. 2012. Viscous dietary fiber reduces adiposity and plasma leptin and increases muscle expression of fat oxidation genes in rats. *Obesity (Silver Spring).* **20**: 349–355.
47. Frier, B. C., R. L. Jacobs, and D. C. Wright. 2011. Interactions between the consumption of a high-fat diet and fasting in the regulation of fatty acid oxidation enzyme gene expression: an evaluation of potential mechanisms. *Am. J. Physiol. Regul. Integr. Comp. Physiol.* **300**: R212–R221.
48. Sugden, M. C., and M. J. Holness. 2003. Recent advances in mechanisms regulating glucose oxidation at the level of the pyruvate dehydrogenase complex by PDKs. *Am. J. Physiol. Endocrinol. Metab.* **284**: E855–E862.
49. Jeoung, N. H., and R. A. Harris. 2010. Role of pyruvate dehydrogenase kinase-4 in regulation of blood glucose levels. *Korean Diabetes J.* **34**: 274–283.
50. Jeoung, N. H., and R. A. Harris. 2008. Pyruvate dehydrogenase kinase-4 deficiency lowers blood glucose and improves glucose tolerance in diet-induced obese mice. *Am. J. Physiol. Endocrinol. Metab.* **295**: E46–E54.
51. Haemmerle, G., T. Moustafa, G. Woelkart, S. Buttner, A. Schmidt, T. van de Weijer, M. Hesselink, D. Jaeger, P. C. Kienesberger, K. Zierler, et al. 2011. ATGL-mediated fat catabolism regulates cardiac mitochondrial function via PPAR-alpha and PGC-1. *Nat. Med.* **17**: 1076–1085.
52. Ong, K. T., M. T. Mashek, S. Y. Bu, A. S. Greenberg, and D. G. Mashek. 2011. Adipose triglyceride lipase is a major hepatic lipase that regulates triacylglycerol turnover and fatty acid signaling and partitioning. *Hepatology.* **53**: 116–126.
53. Obrowsky, S., P. G. Chandak, J. V. Patankar, S. Povoden, S. Schlager, E. E. Kershaw, J. G. Bogner-Strauss, G. Hoefler, S. Levak-Frank, and D. Kratky. 2013. Adipose triglyceride lipase is a TG hydrolase of the small intestine and regulates intestinal PPARalpha signaling. *J. Lipid Res.* **54**: 425–435.
54. Jump, D. B., S. Tripathy, and C. M. Depner. 2013. Fatty acid-regulated transcription factors in the liver. *Annu. Rev. Nutr.* **33**: 249–269.
55. Xu, H. E., M. H. Lambert, V. G. Montana, D. J. Parks, S. G. Blanchard, P. J. Brown, D. D. Sternbach, J. M. Lehmann, G. B. Wisely, T. M. Willson, et al. 1999. Molecular recognition of fatty acids by peroxisome proliferator-activated receptors. *Mol. Cell.* **3**: 397–403.
56. Inagaki, T., P. Dutchak, G. Zhao, X. Ding, L. Gautron, V. Parameswara, Y. Li, R. Goetz, M. Mohammadi, V. Esser, et al. 2007. Endocrine regulation of the fasting response by PPAR-alpha-mediated induction of fibroblast growth factor 21. *Cell Metab.* **5**: 415–425.
57. Schadinger, S. E., N. L. Bucher, B. M. Schreiber, and S. R. Farmer. 2005. PPARgamma2 regulates lipogenesis and lipid accumulation in steatotic hepatocytes. *Am. J. Physiol. Endocrinol. Metab.* **288**: E1195–E1205.
58. Uebanso, T., Y. Taketani, H. Yamamoto, K. Amo, S. Tanaka, H. Arai, Y. Takei, M. Masuda, H. Yamanaka-Okumura, and E. Takeda. 2012. Liver X receptor negatively regulates fibroblast growth factor 21 in the fatty liver induced by cholesterol-enriched diet. *J. Nutr. Biochem.* **23**: 785–790.

59. Ong, K. T., M. T. Mashek, N. O. Davidson, and D. G. Mashek. 2014. Hepatic ATGL mediates PPAR-alpha signaling and fatty acid channeling through an L-FABP independent mechanism. *J. Lipid Res.* **55**: 808–815.
60. Zechner, R., P. C. Kienesberger, G. Haemmerle, R. Zimmermann, and A. Lass. 2009. Adipose triglyceride lipase and the lipolytic catabolism of cellular fat stores. *J. Lipid Res.* **50**: 3–21.
61. Jha, P., T. Claudel, A. Baghdasaryan, M. Mueller, E. Halibasic, S. K. Das, A. Lass, R. Zimmermann, R. Zechner, G. Hoefler, et al. 2014. Role of adipose triglyceride lipase (PNPLA2) in protection from hepatic inflammation in mouse models of steatohepatitis and endotoxemia. *Hepatology*. **59**: 858–869.
62. Li, S., M. S. Brown, and J. L. Goldstein. 2010. Bifurcation of insulin signaling pathway in rat liver: mTORC1 required for stimulation of lipogenesis, but not inhibition of gluconeogenesis. *Proc. Natl. Acad. Sci. USA*. **107**: 3441–3446.
63. Spiekerkoetter, U., and P. A. Wood. 2010. Mitochondrial fatty acid oxidation disorders: pathophysiological studies in mouse models. *J. Inherit. Metab. Dis.* **33**: 539–546.
64. Chakrabarti, P., T. English, J. Shi, C. M. Smas, and K. V. Kandror. 2010. Mammalian target of rapamycin complex 1 suppresses lipolysis, stimulates lipogenesis and promotes fat storage. *Diabetes*. **59**: 775–781.
65. Chakrabarti, P., and K. V. Kandror. 2009. FoxO1 controls insulin-dependent adipose triglyceride lipase (ATGL) expression and lipolysis in adipocytes. *J. Biol. Chem.* **284**: 13296–13300.
66. Badin, P-M., I. K. Vila, K. Louche, A. Mairal, M-A. Marques, V. Bourlier, G. Tavernier, D. Langin, and C. Moro. 2013. High-fat diet-mediated lipotoxicity and insulin resistance is related to impaired lipase expression in mouse skeletal muscle. *Endocrinology*. **154**: 1444–1453.